Preparation and Photocatalytic Properties of Ag/activated Carbon-ZnO Powders

Khanitta Intarasuwan

A Thesis Submitted in Fulfillment of the Requirements for the

Degree of Doctor of Philosophy in Chemistry

Prince of Songkla University

2019

Preparation and Photocatalytic Properties of Ag/activated Carbon-ZnO Powders

Khanitta Intarasuwan

A Thesis Submitted in Fulfillment of the Requirements for the

Degree of Doctor of Philosophy in Chemistry

Prince of Songkla University

2019

Thesis Title Preparation and photocatalytic properties of Ag/activated carbon-ZnO powders

Author Miss Khanitta Intarasuwan

Major Program Chemistry

Major Advisor

……...…….....

(Assoc.Prof.Dr.Pongsaton Amornpitoksuk)

Co-advisor

…….…….....

(Assoc. Prof. Dr. Sumetha Suwanboon)

Examining Committee

…….……...Chairperson

(Asst. Prof. Dr. Pachara Pholnak)

.....…….…….….. Committee

(Assoc.Prof.Dr.Pongsaton Amornpitoksuk)

……...…….….Committee

(Assoc. Prof. Dr. Sumetha Suwanboon)

…….…..Committee

(Asst. Prof. Dr. Uraiwan Sirimahachai)

…….…..Committee

(Dr. Laemthong Chuenchom)

The Graduate School, Prince of Songkla University, has approved this thesis as fulfillment of the requirements for the Doctor of Philosophy in Chemistry.

…….....

(Prof. Dr. Damrongsak Faroongsarng)

Dean of Graduate School

This is to certify that the work here submitted is the result of the candidate's own investigations. Due acknowledgement has been made of any assistance received.

....……..……Signature

(Assoc.Prof.Dr.Pongsaton Amornpitoksuk)

Major Advisor

……..…….Signature

(Khanitta Intarasuwan)

Candidate

I hereby certify that this work has not been accepted in substance for any degree, and is not being currently submitted in candidature for any degree.

……..Signature

(Khanitta Intarasuwan)

Candidate

ชื่อวิทยานิพนธ์ การเตรียมและสมบัติการเร่งปฏิกิริยาทางแสงของผง Ag/activated carbon-ZnO

ผู้เขียน นางสาว ขนิษฐา อินทรสุวรรณ์

สาขาวิชา เคมี

ปีการศึกษา 2562

บทคัดย่อ

งานวิจัยนี้ศึกษาอิทธิพลของชนิดของตัวตกตะกอนที่แตกต่างกัน ($X_2C_2O_4$, X = H, Na, NH_4) ปริมาณของถ่านกัมมันต์ (AC) และปริมาณของโลหะเงิน (Ag) ที่มีผลต่อการเร่งเชิงแสงของผงซิงค์ออกไซด์ (ZnO) เมื่อซิงค์ไอออน (Zn^{2+}) ทำปฏิกิริยากับ $C_2O_4^{2-}$ จะเกิดซิงค์ออกซาเลตไดไฮเดรต ($ZnC_2O_4.2H_2O$) หลังจากทำการเผาสารดังกล่าวที่อุณหภูมิ 500 องศาเซลเซียส เป็นเวลา 1 ชั่วโมง จะได้ ZnO โดย ZnO ที่เตรียมจาก $H_2C_2O_4$ มีพื้นที่ผิวที่สูงสุด และมีความสามารถในการสลายสีย้อมเมทิลีนบลู (MB) และรีแอคทีฟออเรนจ์ (RO) ภายใต้การฉายแสงยูวีได้สูงสุด เมื่อเปรียบเทียบกับ ZnO ที่เตรียมได้จาก $Na_2C_2O_4$ และ $(NH_4)_2C_2O_4$ อย่างไรก็ตาม ZnO มีความสามารถในการสลายสีย้อมต่ำ ภายใต้การฉายแสงช่วงวิสิเบิล ดังนั้นจึงได้ทำการเติม AC และ Ag ใน ZnO ตามลำดับ เพื่อปรับปรุงความสามรถในการเร่งปฏิกิริยาเชิงแสงของคอมโพสิตที่เกิดขึ้น ผลจากการทดลองพบว่า Ag/AC-ZnO สามารถสลายสีย้อม MB และ RO ภายใต้การฉายแสงในช่วงวิสิเบิลโดยไม่มีการเติมสารเติมแต่งใด ๆ ในขณะที่ H_2O_2 เป็นสารเติมแต่งที่สำคัญสำหรับการสลายบิสฟีนอล เอ (BPA) ผลการทดสอบความเป็นพิษที่มีต่อเซลล์ปกติพบว่า เมื่อนำเซลล์ L-929 มาบ่มในสารละลายสีย้อม และ BPA เป็นเวลา 72 ชั่วโมง พบว่าปริมาณการรอดชีวิตของเซลล์ในสารละลายที่ผ่านกระบวนการเร่งเชิงแสงมีค่ามากกว่าในสารละลายก่อนการบำบัดด้วยกระบวนการเร่งเชิงแสง ดังนั้นสามารถจะสรุปได้ว่า ผลิตภัณฑ์ที่เกิดขึ้นหลังจากการเร่งปฏิกิริยาเชิงแสง มีความเป็นพิษต่ำกว่าสารละลายสีย้อมเริ่มต้นหรือโมเลกุล BPA

Thesis Title	Preparation and photocatalytic properties of Ag/activated carbon-ZnO powders
Author	Miss Khanitta Intarasuwan
Major Program	Chemistry
Academic Year	2019

ABSTRACT

This research was studied the influence of type of precipitating agents ($X_2C_2O_4$, X = H, Na or NH_4) and amounts of activated carbon (AC) and metallic silver (Ag) on photocatalytic activity of ZnO. When Zn^{2+} ions reacted with $C_2O_4^{2-}$, $ZnC_2O_4.2H_2O$ was produced as intermediate species and this compound was decomposed to ZnO after calcination at 500 ^oC for 1h. The ZnO prepared from $H_2C_2O_4$ exhibited the highest surface area and showed the highest photocatalytic degradation of methylene blue (MB) and reactive orange (RO) under blacklight irradiation compared to the other ZnOs prepared by $Na_2C_2O_4$ and $(NH_4)_2C_2O_4$. However, this ZnO demonstrated a low activity under visible light irradiation. Thus, the activated carbon (AC) and Ag were added into the ZnO in order to improve the photocatalytic activity of resulting composite. The experimental results showed that the Ag/AC-ZnO can degrade MB and RO under visible light irradiation without any additive while the H_2O_2 was the important additive for degradation of BPA. After exposure of L-929 cells to dye and BPA solution before and after photocatalysis for 72 h, the cell viability after exposure in the solution after photocatalysis was higher than in initial solution. It can conclude that the degraded products after photocatalytic reaction were less toxic than parent dye or BPA molecules.

ACKNOWLEDGEMENT

I would like to express my deep appreciation to my advisor, Assoc. Prof. Dr. Pongsaton Amornpitoksuk, who suggested this research problem, for his kindness, guidance and assistance in reading, correcting and criticizing the manuscript.

I would like to express my profound gratitude to my co-advisor, Assoc. Prof. Dr. Sumetha Suwanboon for the valuable suggestion on my thesis and assistance in reading, correcting and criticizing the manuscript.

I am grateful to my examining committee, Asst. Prof. Dr. Pachara Pholnak of the Department of Physics, Faculty of Science, Thaksin University, Asst. Prof. Dr. Uraiwan Sirimahachai of the Department of Chemistry, Faculty of Science, Prince of Songkla University and Dr. Laemthong Chuenchom of the Department of Chemistry, Faculty of Science, Prince of Songkla University, for the kindness, comment and helpful suggestion.

I would like to thank the Department of Chemistry, Faculty of Science, Prince of Songkla University, for all necessary laboratory facilities used thoughout this research.

I am grateful to the grant funds from PSU Ph.D. Scholarship and the Graduate School, Prince of Songkla University, for the financial supports and laboratory expenses throughout this research.

My deep gratitude is also due to all my friends and staffs who give me their help and shared a hard time with me during my study.

Finally, I would like to express my deepest appreciation to my parents and my husband for great understanding, encouragement and support.

Khanitta Intarasuwan

CONTENTS

CONTENTS (CONTINUED)

LIST OF TABLE

LIST OF FIGURE

LIST OF FIGURE (CONTINUED)

LIST OF FIGURE (CONTINUED)

CHAPTER 1

INTRODUCTION

1.1. Environmental Pollution

Pollution refers to a situation in which there is an excess amount of harmful materials or energies into the environment and leads to negative/undesirable change in the environment or has adversely affects for all living things. Releasing of chemical pollution to environment can make three main kinds of pollution: water pollution, land or soil pollution, and air pollution. Examples of pollution that are caused by the introduction of excess energies into environment are noise pollution, thermal pollution, and light pollution. All types of pollution have adverse affects on human health and wildlife, and put the entire planet in danger.

Water pollution is one of the most serious environmental problems because the clean water is an essential substance for plant and animal including human. One of the main sources of water pollution is the results of human activities: industrialization, domestic activity, and agricultural practices. Textile industry is one of the biggest industries in the word that produces large volume of wastewater. This effluent is highly colored that affects on photosynthesis in submerged aquatic plant and has impact on aquatic life due to low light penetration and oxygen consumption. Some dyes may also undergo degradation to form products that are carcinogenic and highly toxic (Rindle *et al.*, 1975). Thus dyes are a potential hazard to living organisms as shown in Figure 1.1.

Figure 1.1. Fish kill caused by dye contamination in river.
Source: Qamar, *et al*., (2005)

Toxic dyes can cause dysfunction of pancreas, kidneys, liver, dermatitis, and skin irritation as seen in Figure 1.2. It is hence important to safeguard the environment from such contaminant.

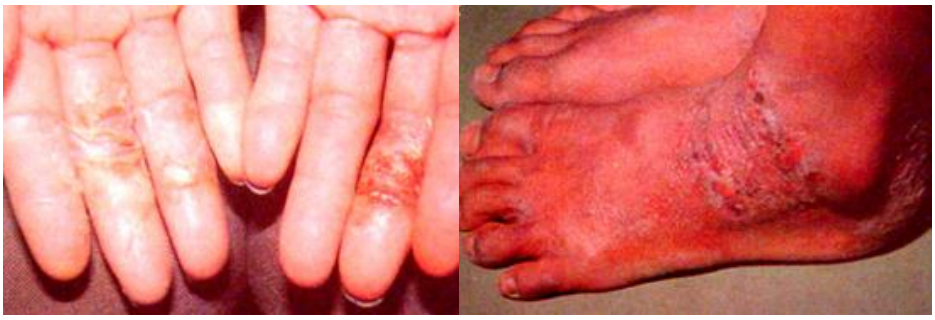

Figure 1.2. Toxicity of dye waste water with human body.

Source: Qamar, *et al*., (2005)

In the present work, it was attempted to degrade organic molecules in aqueous solution. Methylene blue (cationic dye), Reactive orange 16 (anionic dye), and bisphenol A were used as a model of organic pollutant. These dyes and bisphenol A were chosen due to its high chemical, high thermal stability, and biological resistance to degrade by generally, which are attributed to chromosphere group. The importance, application, and hazards of these dyes are presented in Table 1.1.

Table1.1. General information, application, and hazards of methylene blue, reactive orange 16, and bisphenol A.

Pollutant model	General information	Application	Hazards
Methylene blue ($C_{16}H_{18}N_3SCl$)	- the structure as : 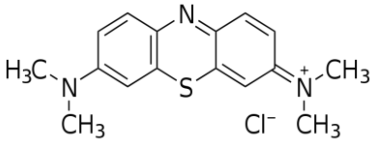 - solid form at room temperature, odorless, dark blue powder, and water soluble. - maximum absorption wavelength at 664 nm. - molar mass = 319.85 g/mole.	- used as a redox indicator in analytical chemistry. - photosensitizer used to create singlet oxygen when exposed to both oxygen and light. - used as a dye to examine DNA or RNA under the microscope or in a gel. - used as an indicator to determine if a cell is alive or not.	- important side effects: vomiting, nausea, stomach upset, and diarrhea. - serious side effects: dizziness, fainting, high fever, fast/irregular/pounding heartbeat, pale/blue skin color, and unusual tiredness. - cause of urine or stool to turn green-blue.

Pollutant model	General information	Application	Hazards
Reactive orange 16 ($C_{20}H_{17}N_3Na_2O_{11}S_3$)	- the structure as : 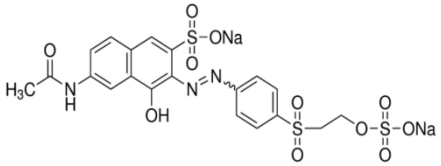 - solid form at room temperature, odorless, dark orange powder, and water soluble - maximum absorption wavelength at 493 nm. - molar mass = 617.54 g/mole.	- used in the textile industry to color cellulosic fibers. - commonly used in the dyeing of fibers, proteins, nylon, acrylic fibers.	- toxicity induced diseases, example skin diseases, allergy, and cancer. - the presence of color in water reduces the transmittance of light which affects the photosynthesis of organism in water**.**

Pollutant model	General information	Application	Hazards
Bisphenol A ($C_{15}H_{16}O_2$)	- the structure as : 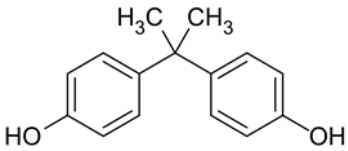 - solid form at room temperature, odorless, colorless powder, and soluble in organic solvents, but slightly soluble in water. - maximum absorption wavelength at 277 nm. - molar mass = 228.29 g/mole.	- starting substance for the synthesis of plastics. - used primarily for the manufacture of polycarbonate plastic and epoxy resins. - used to coatings on the inside of beverage cans and many food, and used to make paper that is highly resistant to heat. - use in baby bottles and infant formula packaging.	- bisphenol A is a substance that destroys the endocrine glands. - It can interfere with hormones in the body. - bisphenol A exposure can affect egg maturation in humans. - It interferes with the hypothalamus glands and the pituitary gland. - affects ovulation and may cause infertility. - bisphenol A exposure to affect cardiovascular problems, including coronary artery heart disease, angina, heart attack, hypertension, and peripheral artery disease.

According to a harmful of dyes and bisphenol A, the wastewater must be treated before discharge to environment. Traditional techniques used for toxic substance removal are listed in Table 1.2.

Table1.2. The advantages and disadvantages for traditional techniques used for toxic substance removal from wastewater.

Techniques	Advantages	Disadvantages
Activated carbon adsorption	- Technically easy method.	- High waste disposal cost. - Difficult to remove the color molecules from the surface of the charcoal. - High cost of reusing activated carbon.
Ozone treatment	- Very strong oxidizer. - Rapid degradation of dye molecules.	- Most of them contain chlorine nitrogen or sulfur is a toxic compound.
Ion exchange	- Very effective process. - If treating heavy metals, they can often be reused again.	- Water will have increased acidity because of the addition of sodium ions into the water and it will make the water unsafe for use.
Membrane filtration	- No phase changes involved, both substance and product still in a liquid state. - The processes can be done at low temperatures. - Low energy consumption in the process.	- Cleaning and regeneration after the process is expensive. - Equipment cost can be high.

Chemical coagulation	- Low cost process.	- There is a change in pollution from one phase to another phase, which may be more toxic at the beginning phase.
Biological treatment	- Low cost process. - In most cases, the dye is absorbed on the sediment.	- Is a process that take a long time.

1.2. Photocatalysis

Photocatalysis is a process that a material as photocatalyst is activated by light or photons and it leads to speed up the rate of a chemical reaction. There are two types of this process, homogeneous photocatalysis; the reactant and the photocatalyst exist in the same phase and heterogeneous photocatalysis; the reactant and the photocatalyst exist in two or more phase in reaction. The heterogeneous photocatalytic reaction has been widely used in water and air treatment because it can be separated from a reaction mixture using a simple method such as filtration and can be effectively recovered. Photocatalytic process is used to degrade toxic organic molecules to CO_2 and H_2O without additional chemical oxidants, because the degradation is assisted by high the hydroxyl radicals ($^{\bullet}OH$) and superoxide anion radicals ($^{\bullet}O_2^-$) generated in the process. Among semiconductors based heterogeneous photocatalysts (TiO_2, SnO_2, CdS, WO_3, ZnO, and others), ZnO has been successfully used to degradation and many organic pollutants consisted of several dyes (Muruganandham, *et al.*, 2005). Furthermore, it has good photoactivity, high chemical stability, commercial availability, and not expensive. Therefore, ZnO is generally used as a photocatalyst for water pollution such as destroy germs in the water, air purification and water purification (Nagaveni, *et al.*, 2004).

The photocatalytic mechanism of ZnO has been summarized in Scheme 1.1. The reaction begins with ZnO being excited with UV ray (E_g of ZnO = 3.37 eV) resulting in the formation of electron-hole pair, Eq.1.1. The photogeneratedelectron in the conduction band, e_{cb}^-, and the positive hole in the valence band, h_{vb}^+, may recombine and reduce further reactions. The $e_{cb}^- - h_{vb}^+$ pair, if they survive from

charge recombination process, will eventually diffuse to the bulk surface and react with other molecules nearby. The e_{cb}^- can react with O_2 molecule adsorbed at the bulk surface of ZnO and after steps will the formation of $^{\bullet}OH$ radical, Eqs.1.2-1.5, that plays an important role in photocatalytic activity. The h_{vb}^+ can to react with H_2O at the bulk surface of ZnO to formation of $^{\bullet}OH$ radical as well, Eq.1.6. The very reactive $^{\bullet}OH$ radical can go on by attacking the dye molecules and organic molecules to degradation them, Eq.1.7. In addition, the h_{vb}^+ itself can attack and degradation dye molecules, Eq.1.8 (Hucine, *et al*., 2009).

$$ZnO + hv \longrightarrow e_{cb}^- + h_{vb}^+ \quad 1.1$$

$$O_{2ads} + e_{cb}^- \longrightarrow {}^{\bullet}O_2^- \quad 1.2$$

$$^{\bullet}O_2^- + H^+ \longrightarrow {}^{\bullet}OOH \quad 1.3$$

$$2\,{}^{\bullet}OOH \longrightarrow H_2O_2 + O_2 \quad 1.4$$

$$H_2O_2 + e_{cb}^- \longrightarrow {}^{\bullet}OH + OH^- \quad 1.5$$

$$H_2O_{ads} + h_{vb}^+ \longrightarrow H^+ + {}^{\bullet}OH \quad 1.6$$

$$Dye + {}^{\bullet}OH \longrightarrow \text{Degradation products} \quad 1.7$$

$$Dye + h_{vb}^+ \longrightarrow \text{Degradation products} \quad 1.8$$

Scheme1.1. Mechanism of ZnO photocatalyst.

1.3. Precipitation method

ZnO powders can be prepared by various methods such as sonochemical, sol-gel, vapor phase deposition and precipitation methods. Various methods of preparation, such as thermal evaporation, chemical vapor deposition (CVD), metal organic chemical vapor deposition (MOCVD). Preparation of ZnO powders via chemical routes without adding catalysts or no templates promising function for the large-scale production of good dispersed materials. Among wet chemical routes, precipitation method has many advantages over the other methods, such as, it can reaction at room temperature and a low cost method. Generally, the ZnO prepared by this method usually occurs through two main mechanisms; (1) direct formation and (2) precursor formation. For the direct formation, the Zn^{2+} ions react with precipitating species to

form the ZnO and this reaction is usually archived under highly alkaline solution or high reaction temperature;

$$Zn^{2+} + \text{precipitating species} \longrightarrow ZnO$$

Indeed, some of precipitating agents cannot produce ZnO when the reaction is complete, but it generates ZnO-precursor which further decompose to ZnO after calcination:

$$Zn^{2+} + \text{precipitating species} \longrightarrow \text{ZnO-precursor} \longrightarrow ZnO$$

From literature, base is very popular precipitating agent that is used for the synthesis of ZnO powder. Examples of bases using as precipitating agent for preparation of ZnO are listed in Table 1.3.

Table 1.3. Selected some precipitating agents for preparation of ZnO.

Reference	Precipitating agent	Procedure
Yujun *et al.*, (2010)	NH_4HCO_3	$ZnSO_4$ solution ↓ - NH_4HCO_3 solution - hydrothermal at 80 ^oC for 3 h. White precipitates ↓ - wash, filter, and dry - calcine at 300, 350, 400, and 500 ^oC for 2 h. Spherical like ZnO nanoparticles

Reference	Precipitating agent	Procedure
Amrut *et al.*, (2012)	NaOH	0.3 g of soluble starch in 100 mL of water ↓ - add 0.1 M of $ZnNO_3$ - stir for 2 h. - add dropwise of 0.2 M NaOH solution White solution ↓ - filter, wash, and dry at 100 ^oC for 2 h. ZnO nanoparticles
Davood *et al.*, (2012)	$(NH_4)_2CO_3$	$Zn(NO_3)_2$ solution ↓ - add $(NH_4)_2CO_3$ solution ZnO precursor ↓ - filter, wash, and dry - anneal at 250, 350, 450, and 500 ^oC for 4 h. ZnO nanoparticles

Reference	Precipitating agent	Procedure
Hongqian *et al.*, (2012)	$NH_3.H_2O$	0.5 M $Zn(NO_3)_2$ solution ↓ - slowly drop 4 M $NH_3.H_2O$ solution Suspension ↓ - stir at 60 ^oC for 30 min ZnO precursors ↓ - filter, wash, and dry at 80 ^oC for 5 h. ZnO precursors ↓ - calcine at 500 ^oC for 1 h. with a heating rate of 5 ^oC/min Flower-like ZnO bunches
Napaporn *et al.*, (2013)	NaOH	100 mL of 0.5 M $(Zn(NO_3)_2.6H_2O$ ↓ - slowly add NaOH solution White precipitates ↓ - wash with DI water - dry at 80 ^oC for 6 h. Needie-like ZnO nanopowders

Reference	Precipitating agent	Procedure
Kanouli *et al.*, (2015)	NaOH	0.100 g $HOOC(CH_2)_4COOH$ ↓ - 0.1960 g $ZnSO_4.7H_2O$ - 0.273 g NaOH - stir for few minutes ↓ White precipitates ↓ - filter, wash with DI water and acetone - dry at ambient for several hours ↓ Sheet with a nanometric thickness of ZnO powders
Rudeerat *et al.*, (2015)	NaOH	NaOH solution ↓ - add dropwise of $Zn(NO_3)_2.6H_2O$ solution - stir for 30 min - cool to room temperature ↓ ZnO precursor ↓ - filter, wash, and dry at 60 ^oC for 24 h. - anneal at 200 ^oC for 2 h. ↓ ZnO nanopowders

Reference	Precipitating agent	Procedure
Darshan *et al.*, (2016)	LiOH	0.11 M solution of $Zn(NO_3)_2.6H_2O$ ↓ - add dropwise of 1 M LiOH solution - stir for 3 h. White solution ↓ - filter, wash with DI water and ethanol - dry at 120 ^oC for 12 h. ZnO nanopowders
Kanchana *et al.*, (2016)	NaOH	5 g $Zn(CH_3COOH)_2.2H_2O$ in 100 mL of DI water ↓ - 5 g NaOH in 100 mL of DI water - add ethanol - stir for 2 h. White colloids ↓ - filter, wash with ethanol and DI water ZnO powders ↓ - dry at 100 ^oC for 4 h. ZnO nanoparticles

Reference	Precipitating agent	Procedure
Pradeev *et al.*, (2016)	NaOH	$ZnCl_2.4H_2O$ solution ↓ - add drop by drop of NaOH solution - stir for 6 h. White precipitate ↓ - dry at 100 ^oC for 6 h. - calcine at 600 ^oC for 2 h. ZnO nanorods

Besides the bases were presented in Table 1.3, the oxalic acid and its salts are interesting precipitating agents for preparation of ZnO because they can recently produce precipitating porous structure. The selected works that used $H_2C_2O_4$ and $Na_2C_2O_4$ as agent to prepare ZnO powders are presented in Table 1.4.

Table 1.4. Examples of preparation of ZnO powders using oxalic acid or oxalate as the precipitating agent.

Reference	Precipitating agent	Procedure
Li *et al.*, (2009)	$Na_2C_2O_4$	15 mL of 0.05 M $Na_2C_2O_4$ solution ↓ - put into a Teflon-lined autoclave - add zinc foil - heat at 140 ^oC for 24 h. - remove zinc foil from solution ↓ White products ↓ - dry at 50 ^oC ↓ ZnO nanowires
Qazi *et al.*, (2012)	$H_2C_2O_4$	0.05 M of $Zn(CH_3CO_2)_2.2H_2O$ solution ↓ - add dropwise of 0.1 M $H_2C_2O_4$ solution - heat at 80 ^oC for 8 h. ↓ White colored precipitate ↓ - wash with methanol and DI water - dry at 60 ^oC ↓ ZnO nanoparticles

Reference	Precipitating agent	Procedure
Zhigang *et al.*, (2012)	$H_2C_2O_4$	5 mM $H_2C_2O_4$ aqueous solution ↓ - 5 mM $ZnSO_4$ aqueous solution - stir at room temperature - centrifuge, wash with DI water and ethanol - dry at 60 ^oC ↓ White powder ↓ - calcine at 450 ^oC to 650 ^oC for 2 h. ↓ ZnO powder
Shang *et al.*, (2013)	$H_2C_2O_4$	128 mL of $ZnSO_4.7H_2O$ solution ↓ - 0.02 mole $H_2C_2O_4$ - stir for 1 h at room temperature - centrifuge and wash several times with DI water - dry at 80 ^oC for several hours ↓ $ZnC_2O_4.2H_2O$ powder precursor ↓ - calcine at 450 ^oC for 2 h. ↓ ZnO nanopowders

Reference	Precipitating agent	Procedure
Ruixia *et al.*, (2014)	$Na_2C_2O_4$	40 mL of 0.035 M $Zn(CH_3COO)_2.2H_2O$ ↓ - add 0.35 M of $Na_2C_2O_4$ solution - stir for 15 min The mixture precursor ↓ - add into a 100 mL Teflon-lined stainless steel autoclave - heat at 70 ^oC for 24 h. - filter, rinse with ethanol and DI water and dry in air ZnO sheet microcrystals

1.4. Heterostructure ZnO composite photocatalyst

A major limitation of achieving high photocatalytic efficiency in ZnO is the rapid recombination of photoinduced charge carriers. Nevertheless, ZnO has wide band gap (E_g = 3.27 eV) and absorbs photon only in the UV region (below 400 nm) that suffers from limitations for sunlight driven photocatalysis because UV light corresponds to only 4-5% of the whole solar spectrum. To improve the photocatalytic activity of ZnO in visible region, several strategies have been tested including the coupling with a narrow band gap materials that can absorb photon in visible light region, for example, semiconductors (Ag_3PO_4, $CuWO_4$, V_2O_5, BiOCl, etc.), metals (Au, Ag, Pt, Fe, Cu, etc.), and non-metals (C, S, N, C_3N_4, etc.).

Many studies confirmed that the deposition of the plasmonic noble metal (eg., Au, Ag, and Pt) on the surface of ZnO can enhance the efficiency of charge transfer and photocatalytic activity towards organic dye decomposition (Lu *et al.*, 2004; Yang *et al.*, 2008). Among these noble metals, Ag is widely used as a promoter to improve the photocatalytic activity of ZnO**.** Under visible light irradiation, plasmon-excited

electron in the Ag can be transferred to the conduction band of adjacent ZnO and the photogenerated charge carriers are efficiently separated, and can enhance the photocatalytic activity. According to a high cost of Ag, many researchers have attempted to modify the surface of ZnO by incorporation of non-metals. There are many works reported that the addition of activated carbon (AC) on the surface of ZnO can increase the photocatalytic activity of the composite because the AC/ZnO has a large surface area and this heterostructure can increase the charge separation between e^-_{CB} and h^+_{VB} (Eman J *et al*., 2016). The potential of AC and Ag for improvement of photocatalytic activity of ZnO are summarized in Table 1.5.

Table 1.5. The potential of AC and Ag for improvement of photocatalytic activity of ZnO.

1.5.1. Heterostructure of AC-ZnO

Author	Photocatalyst	Chemicals	Synthesized condition	Pollutant model	Results
Sobana *et al.*, (2007)	AC-ZnO composite	- Commercial ZnO - Activated carbon	mixed ZnO and activated carbon at different proportion in an aqueous suspension	Direct Blue 53	Under solar irradiation 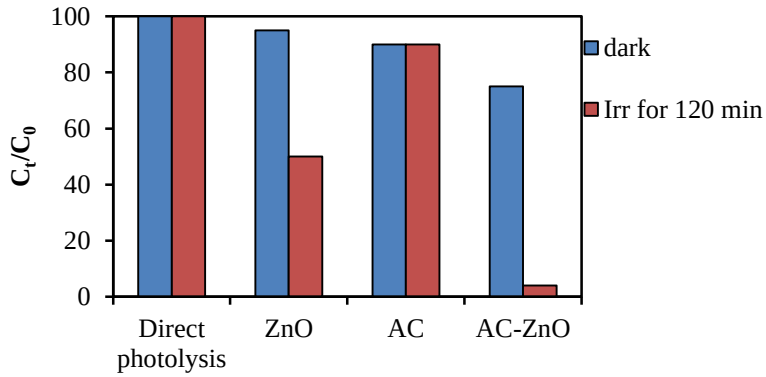
Pulido *et al.*, (2009)	AC-ZnO nanometerial	- Commercial ZnO - Activated carbon	mixed ZnO and AC in aqueous suspension and stirring continuously for 24 h.	Phenol and 2,4 dichlorophenol	- The AC/ZnO nanometerials exhibited higher photocatalytic activity through degradation of phenol and 2,4 dichlorophenol than those of ZnO nanometerials. - Under UV irradiation for 240 min, AC-ZnO can degrade phenol and 2,4 dichlorophenol for 78% and 89%, respectively.

Author	Photocatalyst	Chemicals	Synthesized condition	Pollutant model	Results
Muthirulan *et al.*, (2012)	AC-ZnO composite	- Activated carbon (AC) - Commercial ZnO	Infiltration of a suspension in ethanol of commercial ZnO on the activated carbon in a rotary evaporator under vacuum for 45 min and dried at 110 ^{o}C overnight	Alizarin cyanin green (ACG)	Irradiation for 80 min under UV-ray 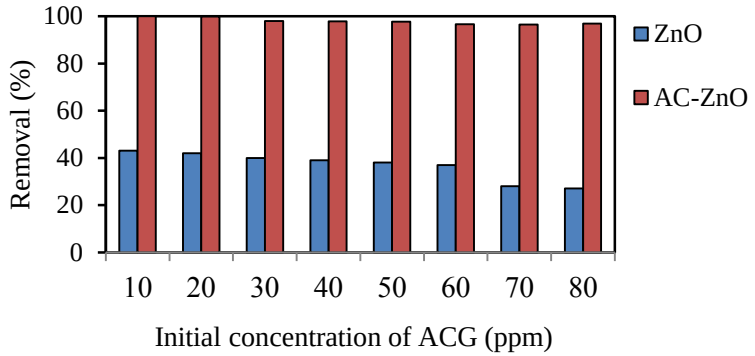
Pankaj *et al* ., (2014)	ZnO-AC	- $Zn(NO_3)_2.6H_2O$ - NaOH - Commercial activated carbon	Co-precipitation method (D.I.water) at 70 ^{o}C for 1 h. - mixed 0.45 M Zn^{2+} solution with 1.0 M NaOH solution and added 1.0 g of AC - dried in air atmosphere at 350 ^{o}C for 4 h.	Malachite green and Congo red dye	Under solar irradiation 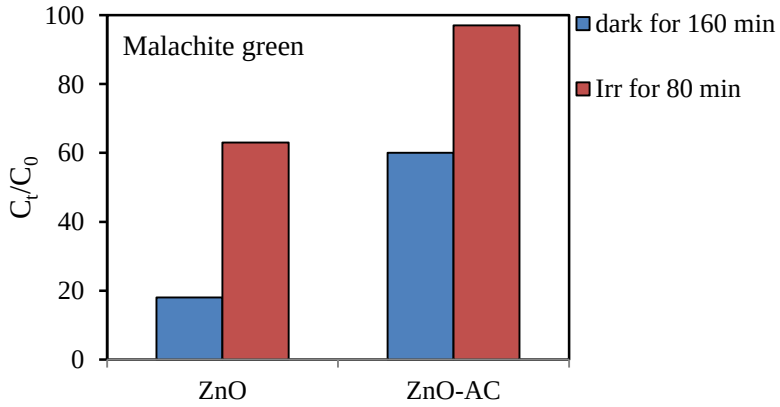

Author	Photocatalyst	Chemicals	Synthesized condition	Pollutant model	Results
					Under solar irradiation 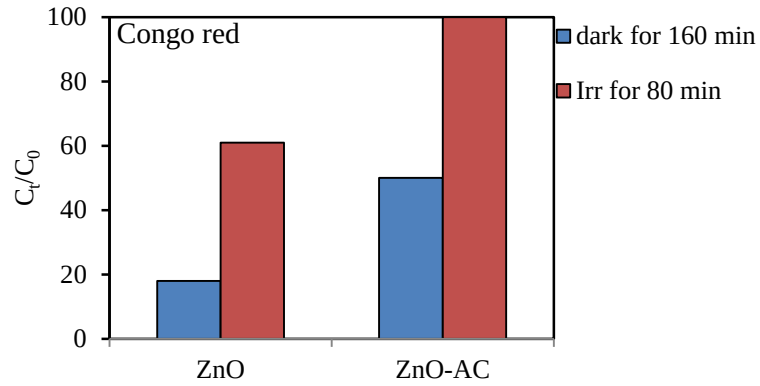
Viet *et al.*, (2017)	Activated carbon fiber (ACF) coated with zinc oxide (ZnO) (ZnO-ACF)	-$Zn(CH_3COO)_2 \cdot 2H_2O$ - NH_4OH - Activated carbon fiber (ACF)	Microwave method (D.I. water) There are three steps: 1. prepared seed solution of ZnO by precipitation method 2. added ACF in the prepared seed solution and stirred under microwave oven for 6 h. 3. dried at 50 ^oC for 24 h.	Tetracycline	Under UV-ray irradiation 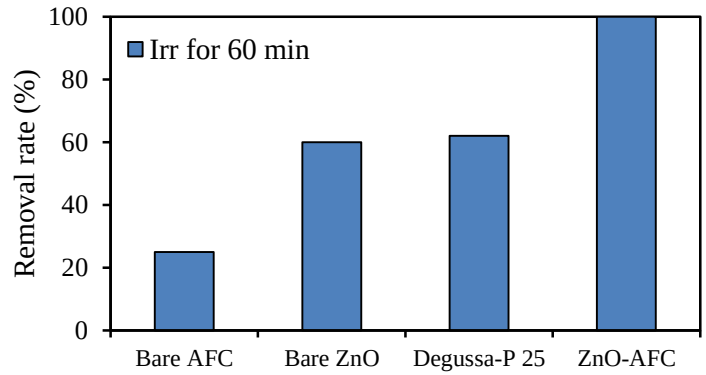

Author	Photocatalyst	Chemicals	Synthesized condition	Pollutant model	Results
					The possible formation mechanism of ZnO in ACF proposed by Eqs. (1.9)-(1.12) $Zn(NH_3)_4^{2+} + 2OH^- \longrightarrow Zn(OH)_2 + 4NH_3$ (1.9) $Zn(NH_3)_4^{2+} + 2OH^- \longrightarrow ZnO + 4NH_3 + H_2O$ (1.10) $Zn(OH)_2 + 2OH^- \longrightarrow Zn(OH)_4^{2-}$ (1.11) $Zn(OH)_4^{2-} \longrightarrow ZnO + H_2O + 2OH^-$ (1.12) The photocatalytic reactions are represented by the following Eqs. (1.13)-(1.17) Semiconductor + hν → electrons from conduction band(e^-) + holes from valence band (h^+) (1.13) $e^- + O_2 \longrightarrow {}^{\bullet}O_2^-$ (1.14) $h^+ + H_2O \longrightarrow H^+ + {}^{\bullet}OH$ (1.15) $h^+ + OH- \longrightarrow {}^{\bullet}OH$ (1.16) $OH/{}^{\bullet}O_2^- +$ organic pollutants → final products (CO_2, H_2O) (1.17)

1.5.2. Heterostructure of Ag/ZnO

Author	Photocatalyst	Chemicals	Synthesized condition	Pollutant model	Results
Zhizhong *et al.*, (2012)	Ag/ZnO flower (ZnO Fl)	- $Zn(CH_3COO)_2 \cdot 2H_2O$ - $Zn(NO_3)_2 \cdot 6H_2O$ - Ammonium hydroxide - $AgNO_3$	Simple photoreduction method - used xenon lamp (50 W) for 0.5h. - calcined at 450 ^oC for 0.5 h.	Rhodamine B	Under visible light irradiation (xenon lamp) 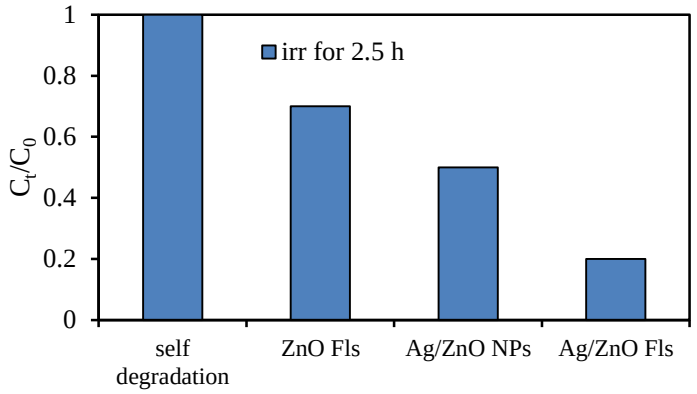 <u>Photocatalytic mechanism</u> $Ag + h\nu \longrightarrow Ag^*$ (1.18) $Ag^* + ZnO \longrightarrow Ag^{\bullet+}\ ZnO_{(e-)}$ (1.19) $ZnO_{(e-)} + O_2 \longrightarrow ZnO + {}^{\bullet}O_2^-$ (1.20) ${}^{\bullet}O_2^- + H^+ \longrightarrow {}^{\bullet}OOH$ (1.21) ${}^{\bullet}OOH + ZnO_{(e-)} + H \longrightarrow H_2O_2 + ZnO$ (1.22) $H_2O_2 + ZnO_{(e-)} \longrightarrow {}^{\bullet}OH + OH^- + ZnO$ (1.23) $RhB + {}^{\bullet}OH$ (or ${}^{\bullet}OOH$) $\longrightarrow$ Photocatalytic products (1.24)

Author	Photocatalyst	Chemicals	Synthesized condition	Pollutant model	Results
Alma *et al.*, (2014)	Ag/ZnO	- ZnO nanoagglomerates - AgNPs	- Photodeposition method (PD) UV lamp for 80 ^{o}C for 8 h. - Impregnation method (IMP) at 300 ^{o}C for 1h.	Bisphenol-A	Under UV-ray irradiation (3UVTM lamp) 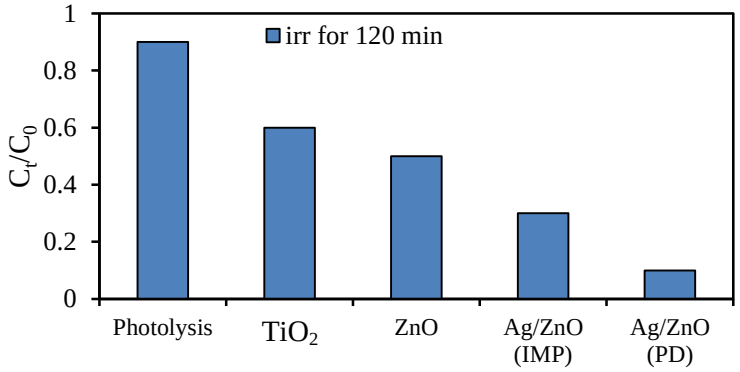
Hongiu *et al.*, (2015)	Ag-ZnO hetero structure	- $Zn(CH_3COO)_2 \cdot 2H_2O$ - $AgNO_3$ - PVP (M.W. = 20,000)	Solvothermal process (Ethanol) - mixed 1.9 mmol Zn^{2+} solution with 0.1 mmol Ag^{+} solution - transferred into a teflon-lined stainless steel autoclave (at 100 ^{o}C for 24 h.)	Rhodamine B (RhB)	Under direct sunlight 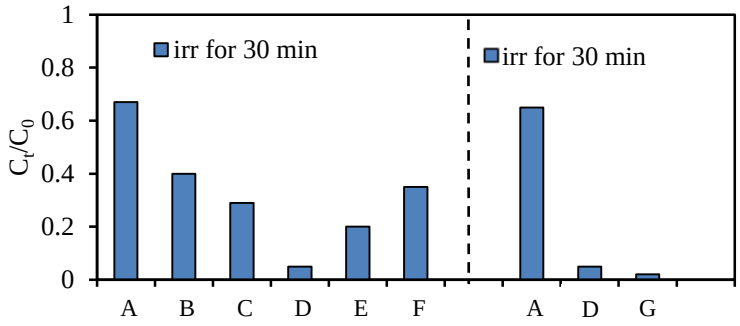 A = ZnO, B = 1% Ag-ZnO, C = 3% Ag-ZnO, D = 5% Ag-ZnO, E = 7% Ag-ZnO, F = 10% Ag-ZnO, G = 5% Ag-ZnO-PVP

Author	Photocatalyst	Chemicals	Synthesized condition	Pollutant model	Results
Houcine *et al.*, (2015)	Mesoporous Ag/ZnO nanocrystals	-$Zn(CH_3COO)_2 \cdot 2H_2O$ - $AgNO_3$ - block copolymer surfactant	Sol-gel method for prepared ZnO (ethanol) - mixed 1.6 g of the block copolymer surfactant with 2.3 mL of CH_3COOH and 0.74 mL HCl - added 2.4 g of Zn^{2+} - calcined at 450 ^oC for 4 h. Photoreduction method for prepared Ag/ZnO (stirred for 12 h under UV illumination and dried at 110 ^oC overnight)	Methylene blue	Under visible light irradiation (250 W visible lamps) 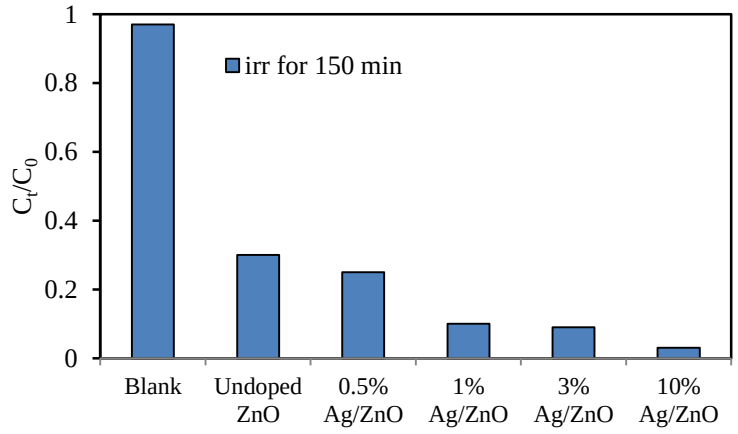 <u>Photocatalytic mechanism</u> 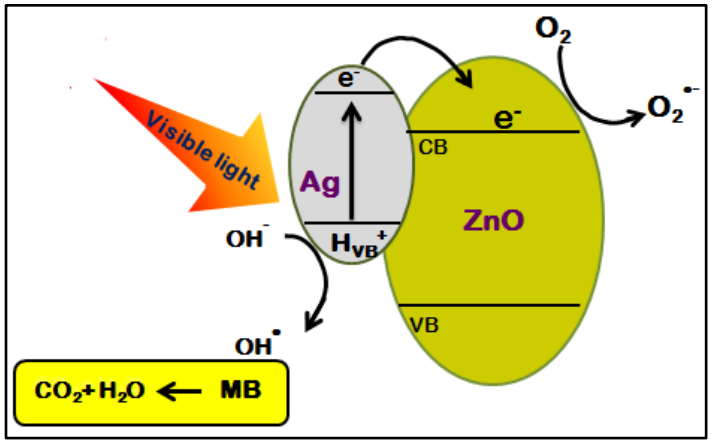

Author	Photocatalyst	Chemicals	Synthesized condition	Pollutant model	Results
Xiaodong *et al.*, (2017)	Flower-like Ag/ZnO	-$Zn(CH_3COO)_2 \cdot 2H_2O$ - $AgNO_3$ - NaOH - $C_6H_8O_7 \cdot H_2O$	Hydrothermal (Ethanol/Water = 1/5 %v/v) - mixed 0.02 mol Zn^{2+} solution with Ag^+ solution - added 10 M NaOH - transferred into a teflon-lined stainless steel autoclave (at 150 °C for 15 h.) - dried at 120 °C for 12 h. - calcined at 500 °C for 2 h.	Methylene blue	Under visible light irradiation (450 W xenon lamp) 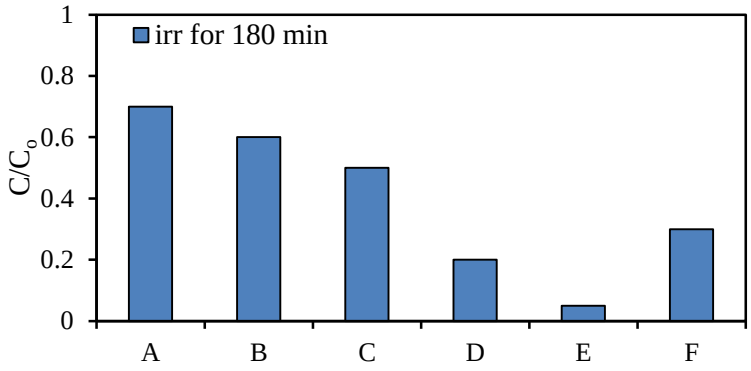 ZnO = A, Ag/Zn ratio (1/50, 1/40, 1/30, 1/20, and 1/10) = B, C, D, E, F respectively <u>Photocatalytic mechanism</u> 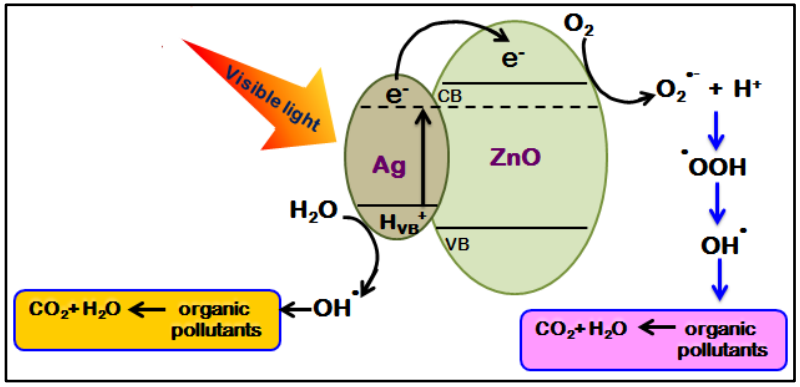

Author	Photocatalyst	Chemicals	Synthesized condition	Pollutant model	Results
Sze Mun *et al.*, (2018)	Flower-like ZnO (Ag/ZnO) micro/ nanostructure	- $Zn(NO_3)_2$ $.6H_2O$ - NaOH - $AgNO_3$	Co-precipitation process for prepared ZnO (D.I. water) - mixed 0.1 M Zn^{2+} solution with 0.1 M NaOH solution - refluxed at 65 ^oC for 8 h. Photoreduction method under sunlight for deposited Ag on surface ZnO (light intensity of 5.7 x 10^5 lux for 2 h.)	Fast Green dye	Under visible light irradiation (45 W compact fluorescent lamp) 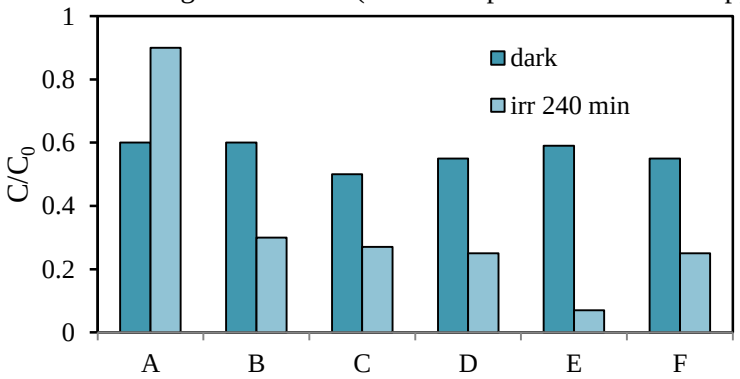 A = photolysis, B = commercial TiO_2, C = pure ZnO, D, E and F is Ag/ZnO (2.5, 5 and 10 %wt Ag, respectively.) <u>Photocatalytic antibacterial activity using E. coli</u> 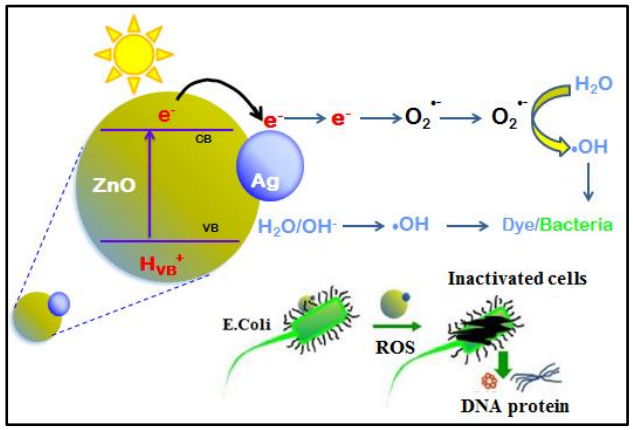

1.5.3. Ag/AC-ZnO composites

Author	Photocatalyst	Chemicals	Synthesized condition	Pollutant model	Results
Bishweshwas *et al.*, (2016)	Ag-ZnO/carbon	- $Zn(NO_3)_2.6H_2O$ - $AgNO_3$ - Carbon nanofiber - Bis-hexamethy-lene triamine	Hydrothermal (D.I.water) - mixed 25 mg of carbon nanofiber with 0.75 g of Zn^{2+} and 20 mg of $AgNO_3$ - transferred into a teflon crucible (at 140 ^oC for 2 h.)	Methylene blue	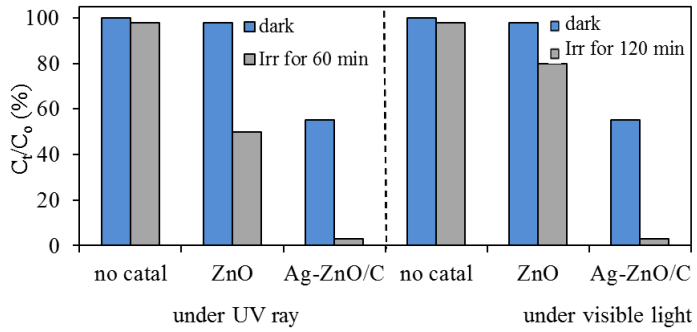
Xiaohua *et al.*, (2017)	Ag/ZnO@C	- $Zn(NO_3)_2.6H_2O$ - $C_6H_5Na_3O_7.2H_2O$ - $AgNO_3$	Hydrothermal (D.I.water) - mixed 3.7 g of Zn^{2+} with 1.5 g of sodium citrate and 0.01 g of carbon spheres - added 0.1 M NaOH and 0.1 M of Ag^+ solution	Reactive Black (GR) and metronidazole	Reactive Black GR 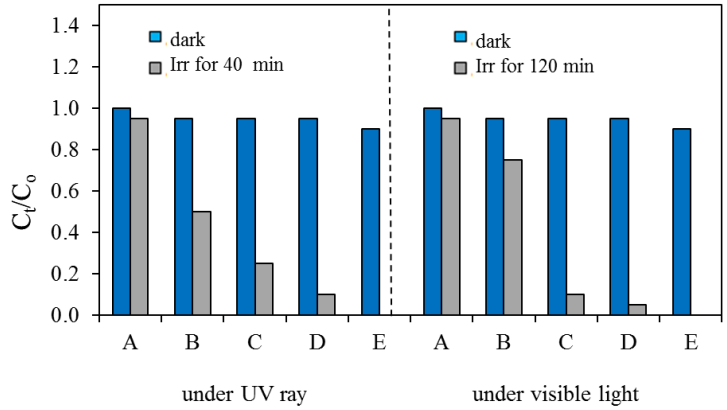

			- transferred into a teflon-lined stainless steel autoclave (at 100 ^{o}C for 10 h.)		Metronidazole 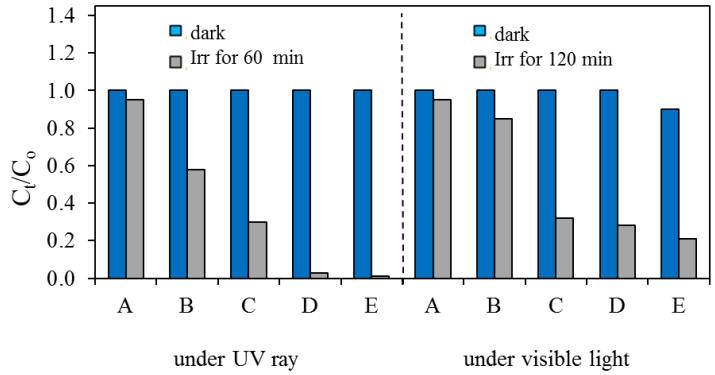 A= blank, B= ZnO, C= ZnO@C, D= Ag/ZnO and E= Ag/ZnO@C <u>Under UV irradiation</u>: $ZnO + hv \rightarrow ZnO(h^{+}_{VB}, e^{-}_{CB})$ $ZnO(e^{-}_{CB}) \rightarrow CS(e^{-})$ $ZnO(e^{-}_{CB}) \rightarrow Ag(e^{-})$ $Ag(e^{-}) + O_2 \rightarrow {}^{\bullet}O_2^{-} \rightarrow {}^{\bullet}OH$ $ZnO(h^{+}_{VB}) + HO^{-} \rightarrow {}^{\bullet}OH$ <u>Under visible light irradiation</u>: $CS(e^{-}) + hv \rightarrow ZnO(e^{-}_{CB})$ $Ag(e^{-}) + hv \rightarrow ZnO(e^{-}_{CB})$ $ZnO(e^{-}_{CB}) + O_2 \rightarrow {}^{\bullet}O_2^{-} \rightarrow {}^{\bullet}OH$

1.5. Research objectives

1. To study the effect of $X_2C_2O_4$ (X = H, Na, NH_4) as the precipitating agent on the photocatalytic activity of ZnO powders under blacklight irradiation.

2. To study the effect of activated carbon (AC) and Ag on the photocatalytic activity of ZnO powders under visible light irradiation.

CHAPTER 2

EXPERIMENTAL METHOD

2.1. Chemicals and Reagents

Chemicals and reagents used in this work were purchased from various suppliers as presented in Table 2.1 and were used as received without further purification.

Tabel 2.1. List of chemicals and reagents.

Chemicals and reagents	Suppliers
Zinc nitrate hexahydrate ($Zn(NO_3)_2.6H_2O$) AR grade	Sigma – Aldrich, Germany.
Oxalic acid dihydrate ($C_2H_2O_4.2H_2O$), AR grade	Merck, Germany.
Sodium oxalate ($Na_2C_2O_4$), AR grade	UNILAB, Australia.
Ammonium oxalate ($(NH_4)_2C_2O_4.H_2O$)	UNILAB, Australia.
Activated charcoal (Powed extra pure), Quality reagent chemical product	QRëC, New Zealand.
Zinc oxide (ZnO), AR grade	Sigma – Aldrich, Germany.
Sodium hydroxide (NaOH), AR grade	Merck, Germany.
Silver nitrate ($AgNO_3$), AR grade	Merck, Germany.
Hydrogen peroxide (H_2O_2), AR grade	Merck, Germany.
Ammonium hydroxide (NH_4OH), AR grade	J.T.Baker, USE.
D(+) – Glucose monohydrate ($C_6H_{12}O_6.H_2O$), AR grade	Riedel – de Haen AG, Germany.
Methylene blue ($C_{16}H_{18}N_3ClS.2H_2O$), AR grade	UNILAB, Australia.
Reactive orange 16 ($C_{20}H_{19}N_3O_{11}S_3\ Na_2$), AR grade	Sigma – Aldrich, Germany.
Bisphenol A ($C_{15}H_{16}O_2$), AR grade	Sigma – Aldrich, Germany.

2.2. Instruments and Equipments

1. X – ray diffractometer, XRD, PHILIPS X' Pert MPD.
2. Scanning electron microscope, SEM, Quanta 400, FEI.
3. UV – visible diffuse reflectance spectrometer (DRS), UV – 2450, Shimadzu.
4. UV – visible Spectrometer, Lambda 25, Perkin Elmer.
5. Transmission electron microscope, TEM, JEM 2010, JEOL.
6. Fourier transform infrared spectrophotometer, FTIR, Spectrum BX, Perkin Elmer.
7. Thermal gravimetric analyzer, TGA7, Perkin Elmer.
8. Liquid chromatography – mass spectrometry, LC – MS, 2690 – LCT, waters, Micromass.
9. Surface area analyzer, Autosorb 1 MP, Quantachrome.
10. Analytical balance, Mettler Toledo, PL403 Precision Balance.
11. Oven, Memmert, UNB 400.
12. Furnace, Carbolite RWF 1300.
13. Centrifuge, EBA 20, Hettich.
14. Magnetic stirrer, Jenway 1000, JENWAY.
15. Wooden box (40 cm x 70 cm x 40 cm) with three tubes of 18 W blacklight fluorescent lamps used as UV – light source. Wooden compartment (75 cm x 75 cm x 75 cm) with a 35 W Xe – lamp used as visible light source.

2.3. Methods

This research was can be divided into 2 parts; (1) preparation and characterization of ZnO, AC-ZnO, and Ag/AC-ZnO by soft chemical route using three different oxalate sources and (2) photocatalytic studies of ZnO, AC-ZnO, and Ag/AC-ZnO through the degradations of MB, RO, and BPA under UV-ray or visible light irradiation.

2.3.1. Preparation of pure ZnO powders

ZnO powders were synthesized via a precipitation method from three different precipitating agents ($H_2C_2O_4$, $Na_2C_2O_4$ and $(NH_4)_2C_2O_4$). A solution of 0.25 M $Zn(NO_3)_2.6H_2O$ was prepared by addition of 1.4874 g $Zn(NO_3)_2.6H_2O$ into 20 mL of distilled water. 0.010 mole of $X_2C_2O_4$ (X = H, Na or NH_4) was dissolved in 60 mL of distilled water. Zinc oxalate precusors were prepared by mixing the $Zn(NO_3)_2.6H_2O$

and $X_2C_2O_4$ solutions together under vigorous stirring and then these solutions were heated at 70 ^oC for 1 h. After being cooled, the resulting product was separated, washed three times with distilled water, and dried at 100 ^oC for 1 h in a hot air oven. Finally, the as-prepared powders were calcined at 500 ^oC for 1 h in a muffle furnace.

2.3.2. Preparation of AC-ZnO powders

AC-ZnO powders were prepared by mixing a 20 mL of 0.25 M $Zn(NO_3)_2.6H_2O$ with a 60 mL of 0.010 mole $H_2C_2O_4.2H_2O$ containing various amounts of activated carbon (0.01 g , 0.02 g and 0.03 g). This mixture was heated at 70 ^oC under vigorous stirring for 1 h. After the resulting mixture was cooled to ambient temperature, it was collected by filtration, washed with distilled water three times, and dried at 100 ^oC for 1 h in a hot air oven. Finally, the resulting product was added into a crucible and covered on the crucible with a lid before heating the product at 500 ^oC for 1 h in a muffle furnace.

2.3.3. Preparation of Ag/AC-ZnO powders

Ag deposited on the surface of AC-ZnO powders were prepared by reduction of $[Ag(NH_3)_2]^+$ solution. The $[Ag(NH_3)_2]^+$ solution was prepared by the dropwise addition of 1 M NaOH into the $AgNO_3$ solution to produce brown solid of Ag_2O. After that, conc. NH_3 solution was continuously added to this suspension until the solid of Ag_2O was transformed to $Ag(NH_3)_2^+$ complex and observed a clear solution. Finally, 1 g of AC-ZnO powder was added into this solution and followed by the addition of 1 M glucose solution. After this mixture was continuously stirred for 1 h at room temperature, the resulting product was filtered, rinsed with distilled water several times, collected, and dried at 100 ^oC for 1 h in a hot air oven.

2.3.4. Photocatalytic studies

Photocatalytic activities of prepared products were investigated through the degradation of methylene blue (MB), reactive orange 16 (RO), and bisphenol A (BPA) under blacklight or visible light irradiation. Blacklight fluorescent tube and Xe lamp were used as the source of UV-ray and visible light, respectively. 100 and 150 mg of samples were added into 150 mL of $1x10^{-5}$ M of dye solution and 150 mL of 5

ppm bisphenol A in a presence of 3 mL of H_2O_2, respectively. This mixture was stirred in the dark for 30 min to reach adsorption-desorption equilibrium and after that, the lamps were turned on. After irradiation for required interval time, 3 mL of dye or bisphenol A was pipetted, centifugated, and collected in the dark. The concentrations of the remaining dyes or bisphenol A as a function of the illumination time were analyzed by a UV-Vis spectroprotometer. The degradation was calculated by the following equation:

$$\text{Degradation (\%)} = [\ (A_o - A_t) / A_o\ ] \times 100$$

where A_o is the absorbance of initial dye or bisphenol A solution and
A_t is the absorbance of the dye or bisphenol A solution after illumination at the required interval times.

CHAPTER 3

RESULTS AND DISCUSSION

3.1. Properties of synthesized ZnO powder

3.1.1. Structure and morphology

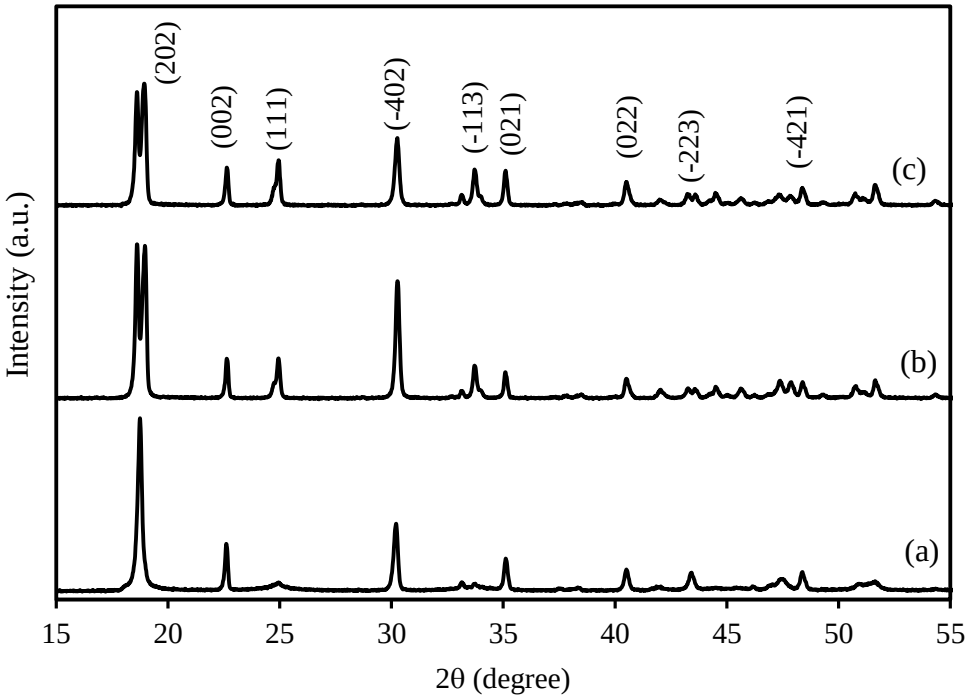

Figure 3.1. XRD patterns of $ZnC_2O_4.2H_2O$ prepared from (a) $H_2C_2O_4$, (b) $Na_2C_2O_4$, and (c) $(NH_4)_2C_2O_4$.

After heating the mixture between $Zn(NO_3)_2$ and $X_2C_2O_4$ (X = H, Na or NH_4) at 70 ^oC for 1 h, the products were characterized by XRD technique. Figure 3.1 displays the XRD patterns of as-synthesize products and it was observed that the diffraction pattern of zinc oxalate precursor prepared from $H_2C_2O_4$ was different from the others. From ICDD database, the diffraction peaks of the as-synthesize products prepared from $H_2C_2O_4$ were matched well with the JCPDS card number 00-025-1029, while the other two as-synthesize products showed the XRD patterns in agreement with the JCPDS card number 00-071-5157. It is a surprise that both JCPDS cards

referred to same compound as $ZnC_2O_4.2H_2O$ crystallizing in the same crystal structure (monoclinic structure with a space group *C2/c*). From literature, the compounds of metal oxalate dihydrate ($M_x(C_2O_4)_y.2H_2O$) have been crystallized in either a monoclinic or an orthorhombic structure but the doublet splitting in the diffraction peak located at 2θ around 18° has always been found in $M_x(C_2O_4)_y.2H_2O$ with the monoclinic structure type (Angermann *et al.*, 2008). Thus, it can be concluded that the $ZnC_2O_4.2H_2O$ prepared from $H_2C_2O_4$ has probably the orthorhombic structure, while the other two compounds are monoclinic structure.

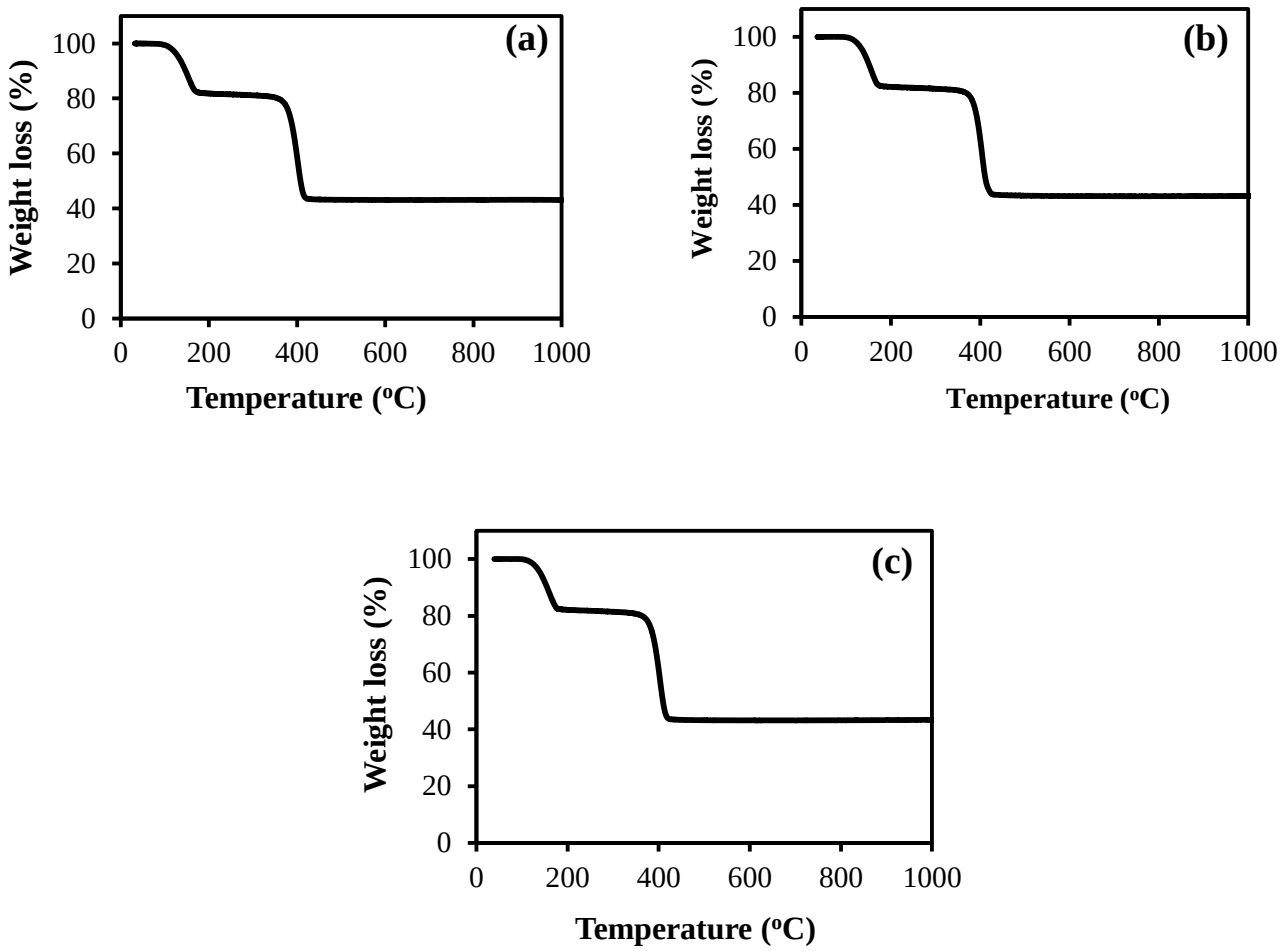

Figure 3.2. TGA curves of $ZnC_2O_4.2H_2O$ precursors prepared from (a) $H_2C_2O_4$, (b) $Na_2C_2O_4$, and (c) $(NH_4)_2C_2O_4$.

Thermal behaviors of all prepared precursors in the temperature range of 30-1000 ^{o}C were investigated by TGA technique at a heating rate of 10 ^{o}C/min. Figure 3.2 shows the TGA curves for three different precursors and they were observed that the TGA curves for all precursors were identical. The first step of weight loss at 100-200 ^{o}C was attributed to the loss of water molecules and the second step in the temperature range 340-420 ^{o}C probably came from the decomposition of ZnC_2O_4 to ZnO.

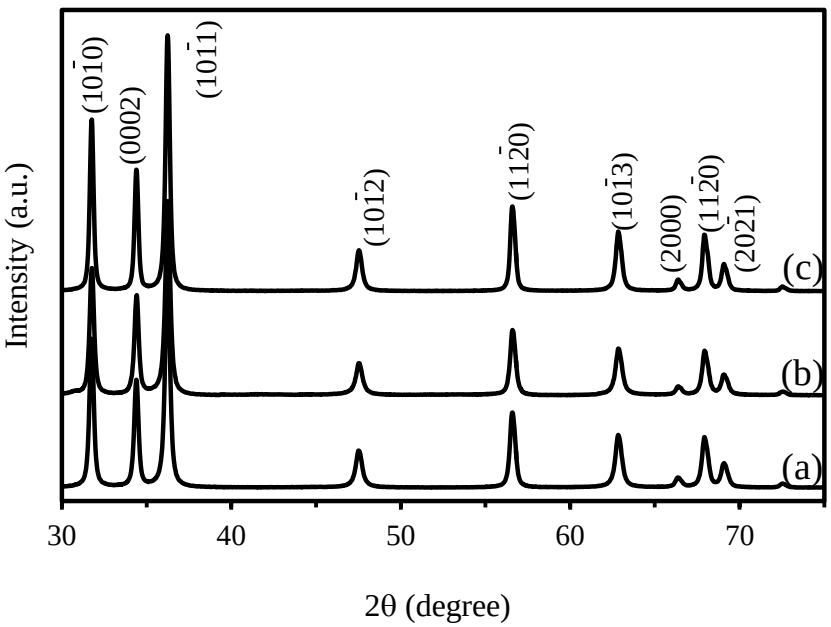

Figure 3.3. XRD patterns of ZnO prepared from (a) $H_2C_2O_4$, (b) $Na_2C_2O_4$, and (c) $(NH_4)_2C_2O_4$ after calcination at 500 ^{o}C for 1 h.

From the TGA results, the temperature of 500 ^{o}C was chosen as the calcination temperature. After the precursors were heated at this temperature for 1 h in the furnace, the XRD patterns of all obtained products prepared by three different precipitating agents were well indexed with hexagonal ZnO (JCPDS number 36-1451) as shown in Figure 3.3. So, it concluded that, after calcination, all products presented the pure phase of ZnO with could be wurtzite structure and without any impurity phase.

Before calcination **After calcination**

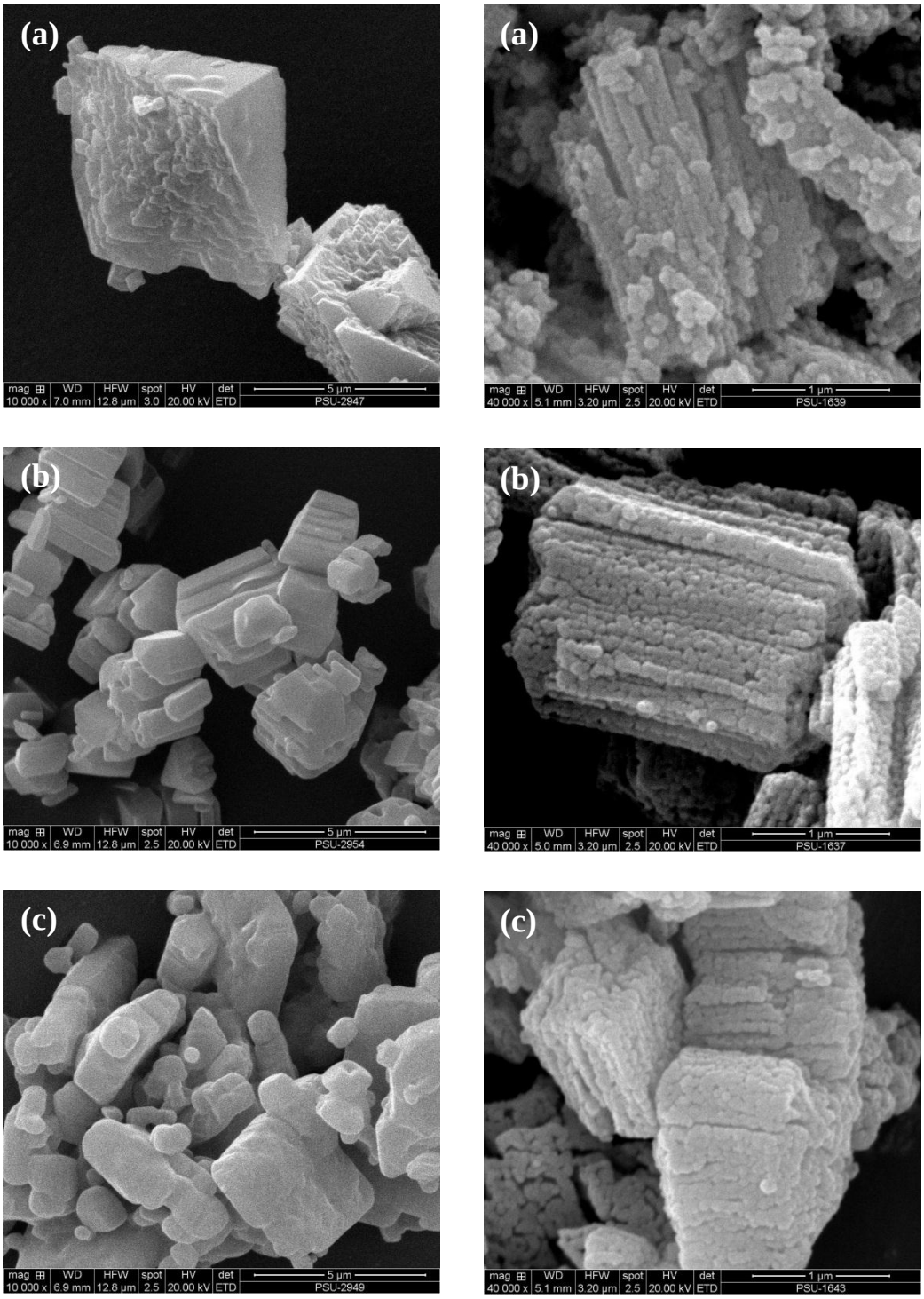

Figure 3.4. SEM images of precursors prepared by (a) $H_2C_2O_4$, (b) $Na_2C_2O_4$, and (c) $(NH_4)_2C_2O_4$ before and after calcination at 500 ^oC for 1 h.

Figure 3.4 demonstrates the SEM images of $ZnC_2O_4.2H_2O$ and ZnO prepared from $X_2C_2O_4$ (X = H, Na or NH_4). The precursor prepared from $H_2C_2O_4$ has a larger size compared with those others prepared from $Na_2C_2O_4$ and $(NH_4)_2C_2O_4$ because the nucleation and growth rates of precursor in $H_2C_2O_4$ solution were lower than that of in $Na_2C_2O_4$ and $(NH_4)_2C_2O_4$ solution. Actually, $Na_2C_2O_4$ and $(NH_4)_2C_2O_4$ are the ionic salts which can fully ionize in water as following:

$$Na_2C_2O_{4(aq)} + H_2O_{(l)} \longrightarrow 2Na^+_{(aq)} + C_2O_4^{2-}{}_{(aq)}$$

$$(NH_4)_2C_2O_{4\,(aq)} + H_2O_{(l)} \longrightarrow 2NH_4^+{}_{(aq)} + C_2O_4^{2-}{}_{(aq)}$$

But, the $H_2C_2O_4$ is a weak acid that shows a partially ionization as following:

$$H_2C_2O_{4(aq)} + H_2O_{(l)} \longleftrightarrow 2H_3O^+{}_{(aq)} + C_2O_4^{2-}{}_{(aq)}$$

After the Zn^{2+} ions were added into oxalate solution, the $ZnC_2O_4.2H_2O$ precursor would be formed as following:

$$Zn^{2+}{}_{(aq)} + C_2O_4^{2-}{}_{(aq)} \longrightarrow ZnC_2O_4.2H_2O_{(s)}$$

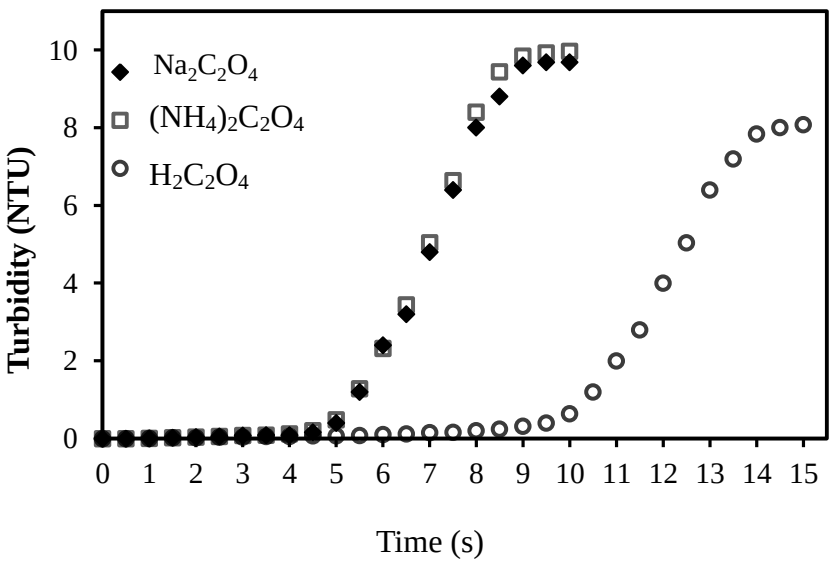

Figure 3.5. Turbidity analyzed during $ZnC_2O_4.2H_2O$ precursor formation in $H_2C_2O_4$, $Na_2C_2O_4$, and $(NH_4)_2C_2O_4$ solutions.

Considering the ionization of three precipitating agents, the concentration of $C_2O_4^{2-}$ species in the $H_2C_2O_4$ solution was lower than that of $Na_2C_2O_4$ and $(NH_4)_2C_2O_4$ solution, so a nucleation of $ZnC_2O_4.2H_2O$ in $H_2C_2O_4$ was the lowest compared with those in $Na_2C_2O_4$ and $(NH_4)_2C_2O_4$ solutions (Figure 3.5). Normally, the high nucleation rate leads to the existence of large particles in good agreement with the SEM images as presented in Figure 3.4. After calcination, the $ZnC_2O_4.2H_2O$ decomposed to ZnO and also released CO_2 and CO according to the following reaction:

$$ZnC_2O_4.2H_2O_{(s)} \longrightarrow ZnO_{(s)} + CO_{2(g)} + CO_{(g)} + 2H_2O_{(g)}$$

This reaction would produce the voids and further generate an agglomerated ZnO nanostructure as shown in Figure 3.4. For $Na_2C_2O_4$ and $(NH_4)_2C_2O_4$, the sizes of $ZnC_2O_4.2H_2O$ and calcinated ZnO did not significantly differ, while the particle size of $ZnC_2O_4.2H_2O$ prepared from $H_2C_2O_4$ was obviously bigger than the ZnO particles after calcination. This probably came from the generated gases during calcination broke down the big precursor into the small agglomerated ZnO nanoparticles as seen in Figure 3.4.

3.1.2. Optical properties

UV-Vis diffuse reflectance spectra of ZnO powders prepared from different precipitating agents are presented in Figure 3.6 (a). ZnO showed high absorption in UV region (λ < 400 nm) owing to the transition of an electron from the valence to the conduction band within ZnO. The estimated optical band gap can be calculated by following equation;

$$\alpha h\nu = A(h\nu - E_g)^n \qquad (3.1)$$

where α is the absorption coefficient which defines as A/0.4, h is the Plank's constant, ν is the photon frequency, A is a constant E_g is the optical band gap and n is ½ for direct allowed transition. The band gap of each sample was estimated by extrapolating the linear portion of the $(\alpha h\nu)^2 - h\nu$ graph until it intercepted the $h\nu$ – axis as presented in Figure 3.6 (b). Using this method, all prepared ZnO powders showed the same E_g value of about 3.22 eV.

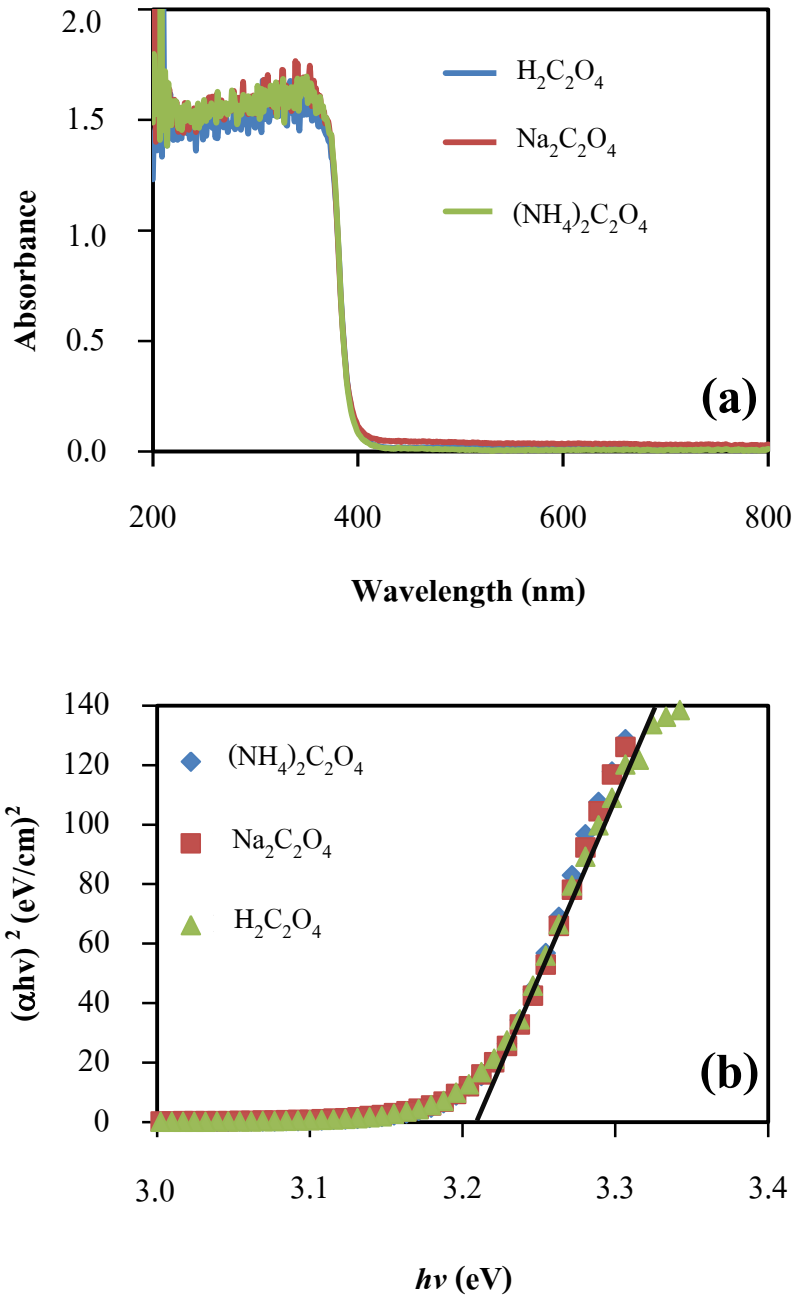

Figure 3.6. (a) DR spectra and (b) a plot between $(\alpha hv)^2$ and hv for ZnO prepared by three different precipitating agents.

3.1.3. Photocatalytic properties of ZnO

The photocatalytic efficiency of prepared ZnO powders was studied through the degradation of MB and RO in aqueous solution under blacklight irradiation. The photocatalytic degradations of MB and RO solutions under blacklight irradiation in the presence of ZnO powders prepared from three precipitating agents were shown in Figure 3.7. A decrease of dye concentration in the dark was attributed to the adsorption of dye on the photocatalyst surface. Reduction of dye by this process is negligible as compared to photocatalytic degradation. The difference in photocatalytic activity of prepared ZnO powders could be attributed to their surface areas. From BET method, the surface areas of ZnO prepared from $Na_2C_2O_4$, $(NH_4)_2C_2O_4$, and $H_2C_2O_4$ were 17.93, 18.63, and 25.85 m^2/g, respectively. The ZnO prepared from $H_2C_2O_4$ showed the highest surface area compared with others. Normally, a high surface area photocatalyst can produce a large population of generated reactive species therefore, the photocatalytic degradation of MB and RO for ZnO prepared from $H_2C_2O_4$ were higher than that of ZnO prepared from $Na_2C_2O_4$ and $(NH_4)_2C_2O_4$.

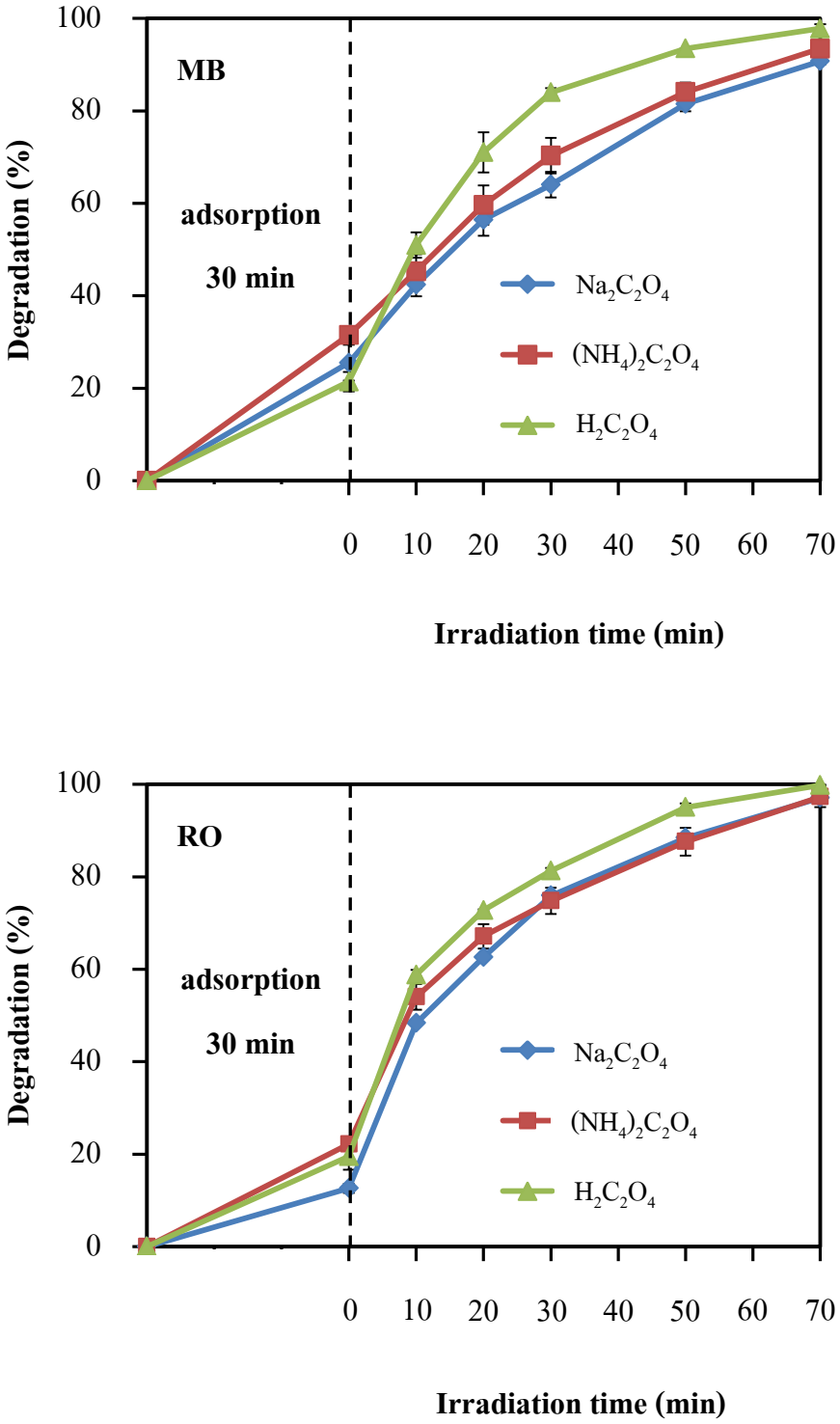

Figure 3.7. Photocatalytic degradation of MB and RO solutions over ZnO prepared by three different precipitating agents under blacklight irradiation.

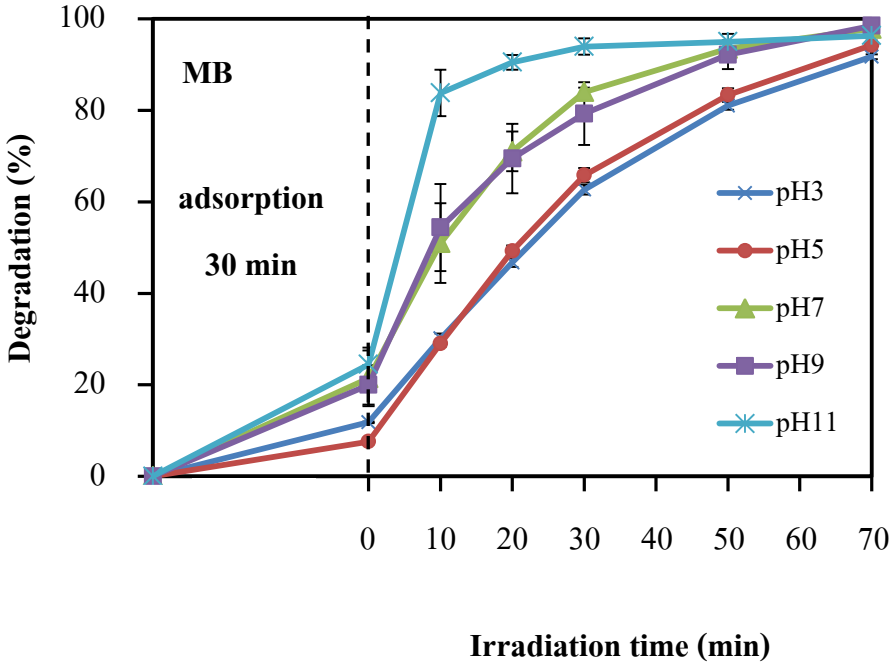

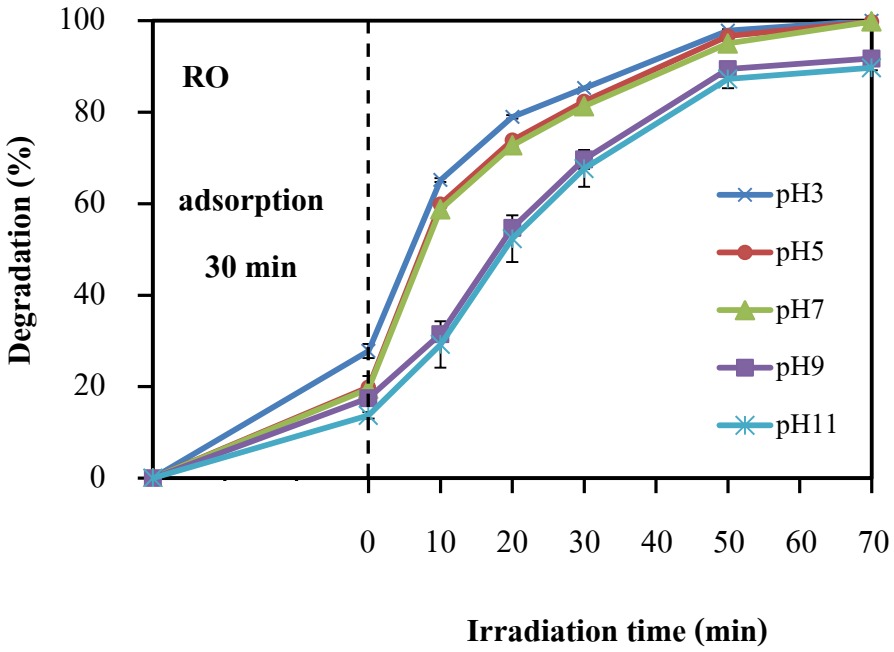

Figure 3.8. Effect of the initial pH on the photocatalytic degradations of MB and RO in the presence of ZnO prepared from $H_2C_2O_4$ as precipitating agent.

The effect of pH on photocatalytic activity of prepared ZnO photocatalyst was evaluated by the degradation of MB and RO dyes at pH of 3, 5, 7, 9, and 11. The experimental results, as presented in Figure 3.7, showed that ZnO prepared from $H_2C_2O_4$ precipitating agent had the highest photocatalytic activity compared with ZnO prepared from $Na_2C_2O_4$ and $(NH_4)_2C_2O_4$, therefore it had been further investigated the effect of pH on its photocatalytic activity. The degradation efficiencies of two dyes under blacklight illumination for 70 min are presented in Figure 3.8. From this figure, it was observed that ZnO in a basic solution showed a better photocatalytic degradation of MB than in an acidic solution. However, the inverse relationship was observed for RO as presented in Figure 3.8. This evidence could be explained by the interaction between ZnO and dye. The pH at the point of zero charge (pH_{pzc}) for ZnO prepared from $H_2C_2O_4$ determined by pH drift method was obtained at a pH ~6.2 as shown in Figure 3.9.

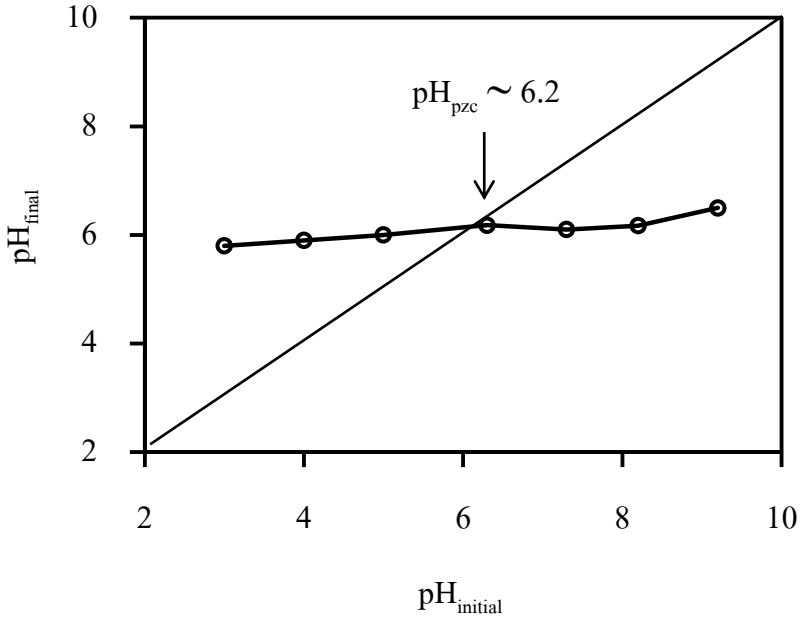

Figure 3.9. Evaluation of the pH_{pzc} of ZnO prepared from $H_2C_2O_4$ by the pH drift method.

In an acidic solution (pH < pH $_{pzc}$), the surface of ZnO was positively charged, so it should repulse with cationic dye leading to reduce its photocatalytic activity. In an alkaline medium (pH > pH_{pzc}), there was an attractive force between the cationic MB dye and the negative charge on the surface of the ZnO. This event can enhance the photocatalytic efficiency of ZnO in the basic solution. In the case of RO, the inverse phenomenon was observed as the RO is an anionic dye. In acidic solution, (pH < pH $_{pzc}$) RO, an anionic dye, reacted with the positive charge on the surface of the ZnO and this event can improve its photocatalytic activity in acidic solution as presented in Figure 3.8.

3.2. Properties of AC-ZnO composite

From previous section (section 3.1), the ZnO prepared from $H_2C_2O_4$ showed the highest photocatalytic degradation of MB and RO under UV light irradiation. So, in this part, an activated carbon (AC) was introduced into this ZnO powder in order to improve the photocatalytic activity of obtained composites under visible light irradiation.

3.2.1. Structure and morphology

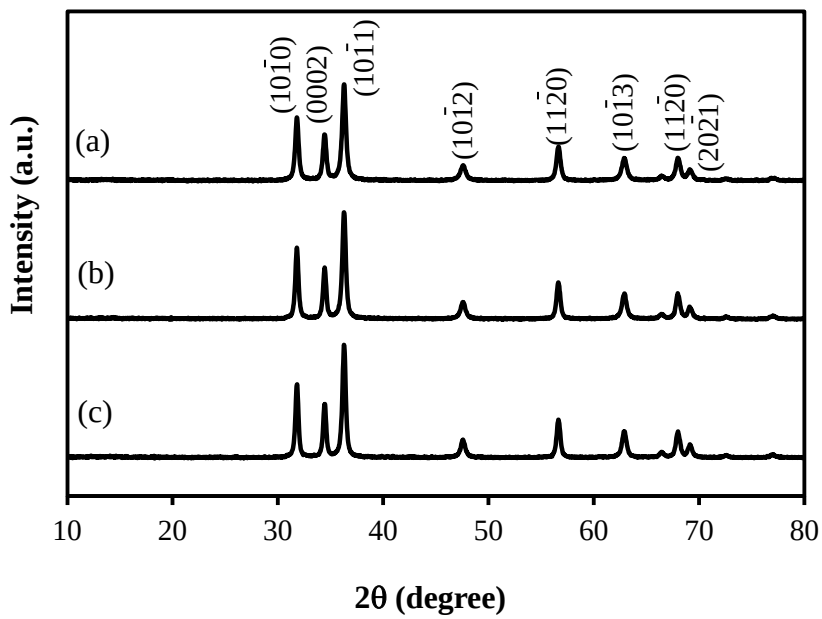

Figure 3.10. XRD patterns of ZnO at various loadings: (a) 0.01 g, (b) 0.02 g and (c) 0.03 g of AC after calcination at 500 ^{o}C for 1 h.

Figure 3.10 shows the XRD patterns of the AC modified ZnO after calcination at 500 ^{o}C for 1 h. It was clearly observed that the XRD patterns of ZnO and all AC-ZnO composites were identical and all diffraction peaks were match well with JCPDS number 36-1451 which is the reference pattern of ZnO crystallizing in wurtzite structure. In the literature, pure AC usually presents two broad peaks at 2θ = 15-35° and 35-50° (Viet *et al.*, 2017). However, the absence of these peaks has been reported in case of low AC loading in the composite sample (Ping Liu *et al.*, 2013).

The morphologies of ZnO and AC-ZnO composite showed the similar shape as presented in Figure 3.11 (a), therefore, the addition of AC in the range of 0.01-0.03 g did not affect the shape of product. As the AC cannot be detected by XRD as shown in Figure 3.10, the EDS technique would be carried out to confirm the existence of AC on the surface of sample. Figure 3.11 (b) displays an EDS spectrum of 0.02AC-ZnO composite. Compared to pure ZnO, AC-ZnO composite showed a higher intensity of C $K\alpha$, so it could be concluded that there was carbon in the AC-ZnO after calcination.

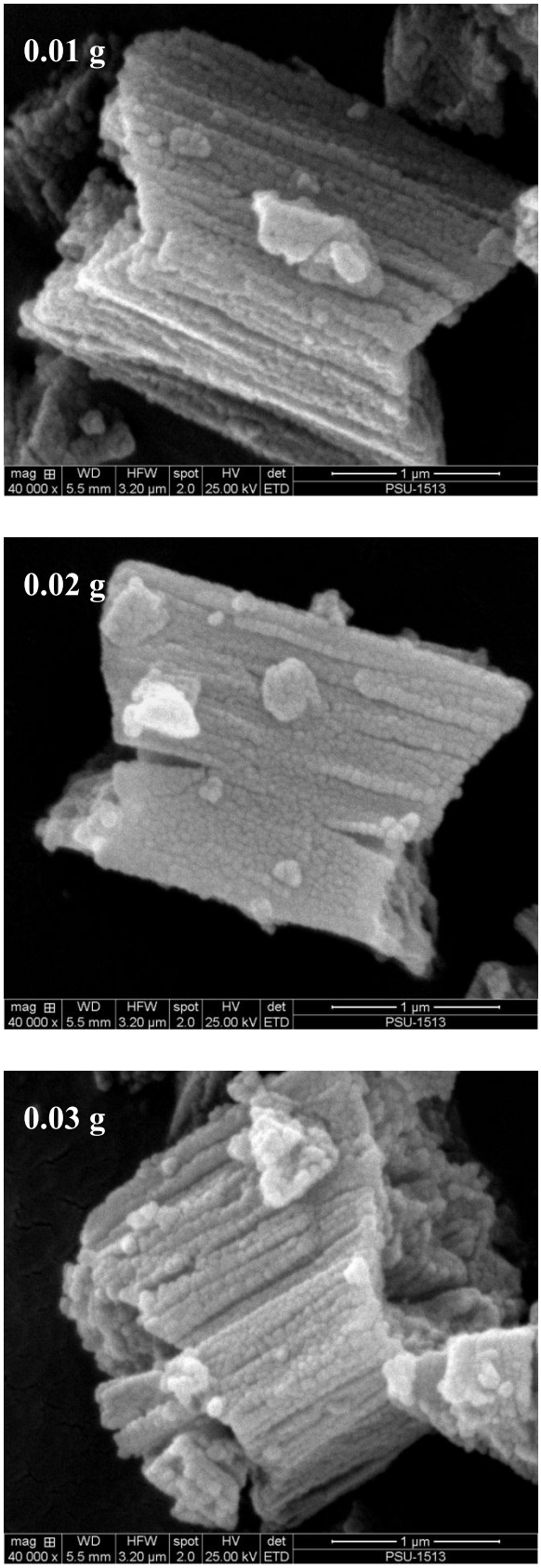

Figure 3.11. (a) SEM images of the AC-ZnO with AC in the range of 0.01-0.03 g.

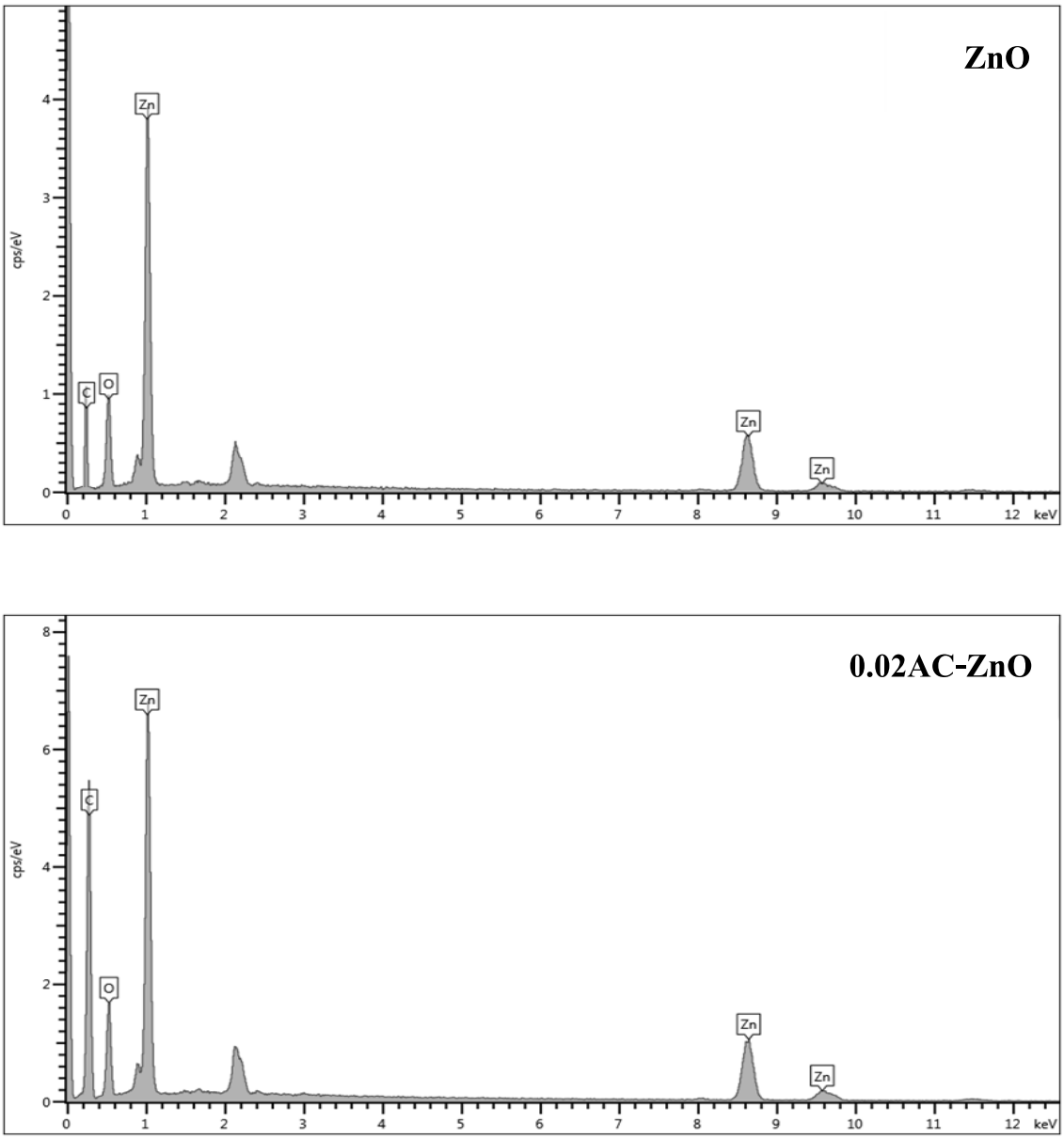

Figure 3.11. (b) EDS spectra of ZnO and 0.02AC-ZnO.

3.2.2. Optical properties

The DR spectra of AC-ZnO composite with various AC loading contents are shown in Figure 3.12 (a). Comparing to ZnO, AC-ZnO composite showed the wideiy broad band in visible region that was attributed to the absorption of AC.

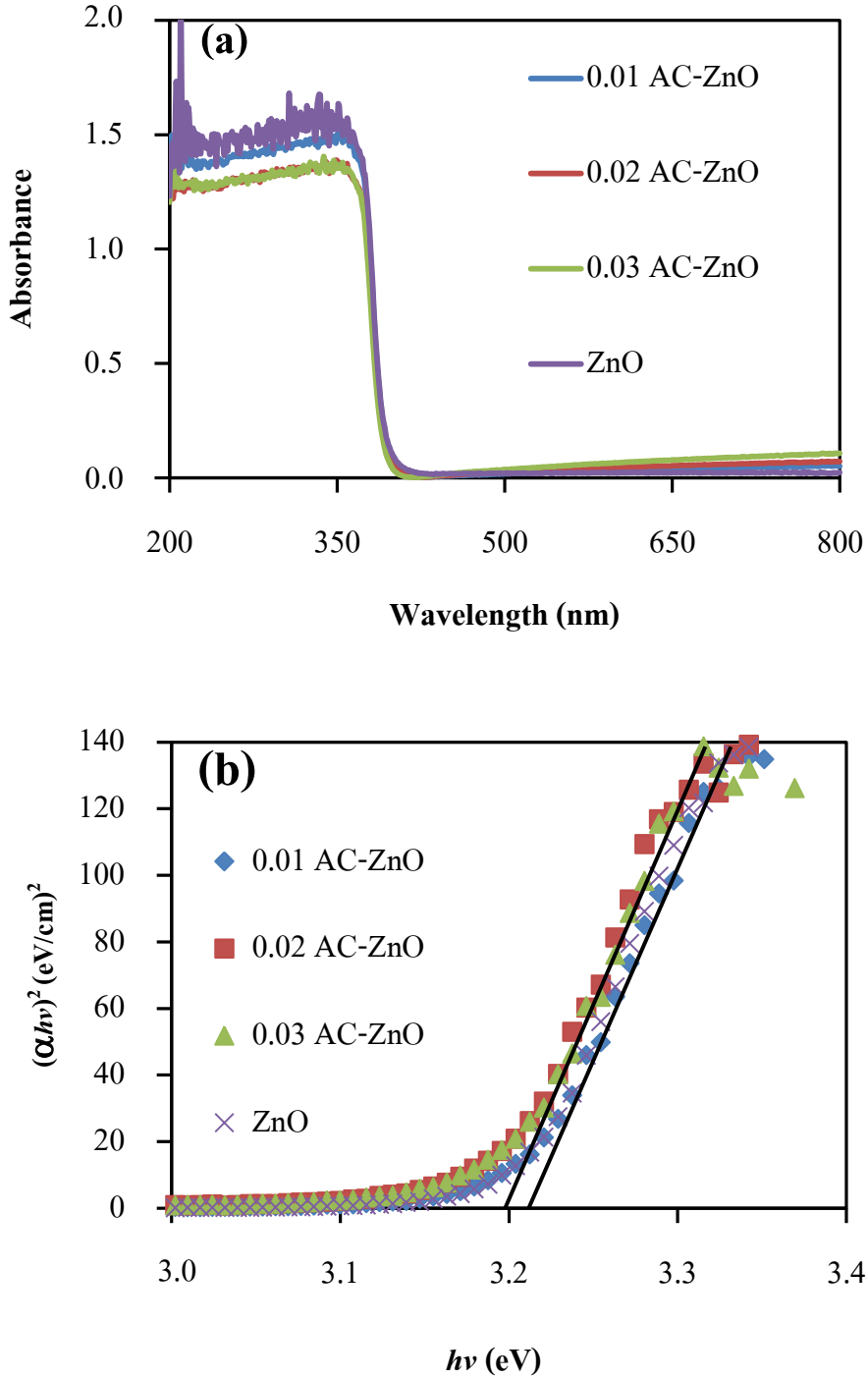

Figure 3.12. (a) DR spectra and (b) the plot between $(\alpha h\nu)^2$ and $h\nu$ for ZnO and AC-ZnO prepared by different AC loading contents.

Figure 3.12 (b) shows the plot of $(\alpha h\nu)^2$ and $h\nu$ for all AC-ZnO conposite powders according to Eq. (3.1). From this Figure, the estimated optical band gap of all prepared AC-ZnO powders showed the same value of about 3.20 eV, that was red-shifted compared with pure ZnO (3.22 eV).

3.2.3. Photocatalytic properties of AC-ZnO

The photocatalytic efficiency of AC-ZnO composite under visible light irradiation was studied using Xe lamp as the visible light source.

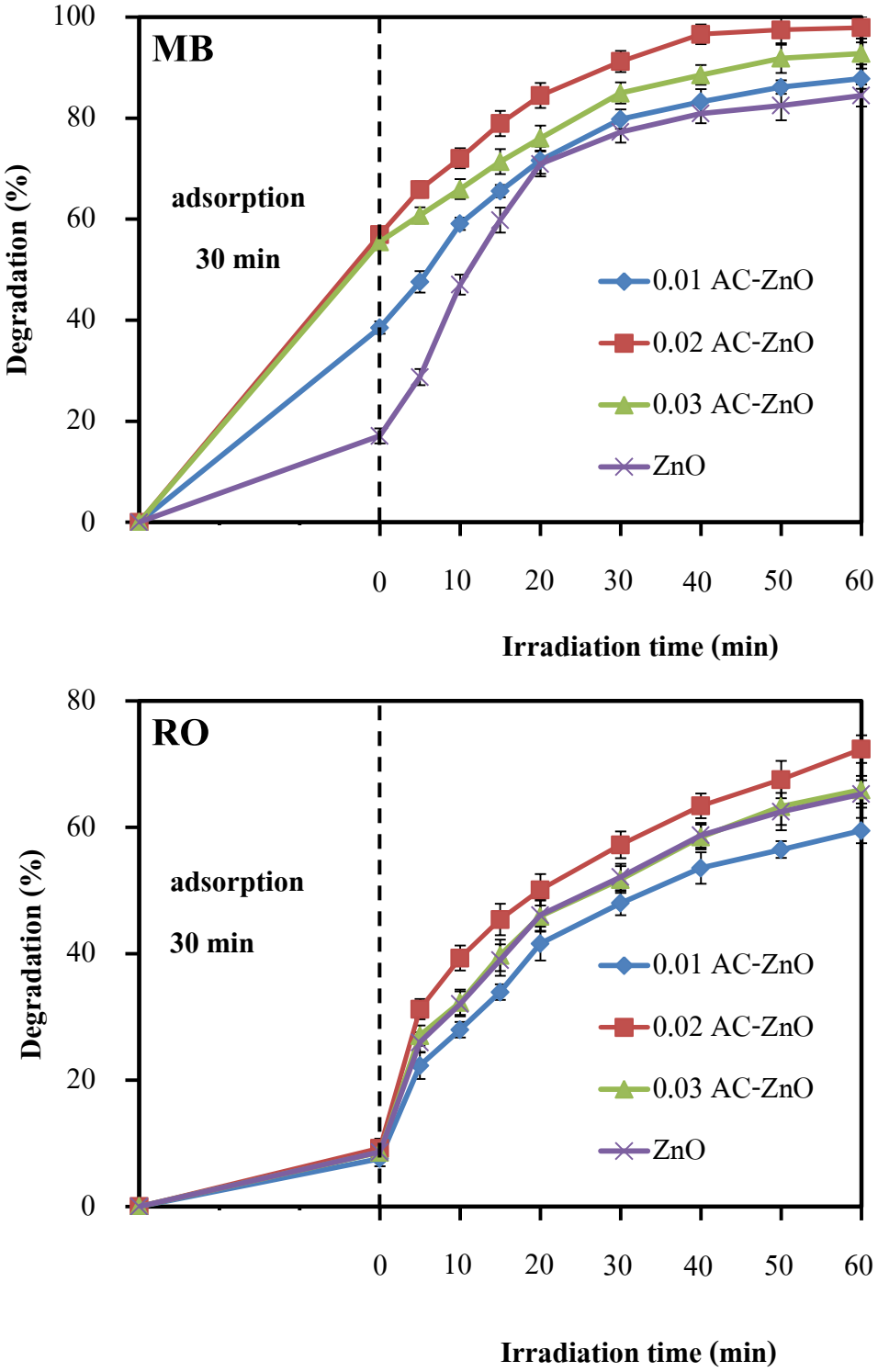

Figure 3.13. The photocatalytic degradation of MB and RO over ZnO and AC-ZnO composite with various AC loadings under visible light irradiation.

The photocatalytic degradation of MB and RO over ZnO and AC-ZnO with various AC loading contents under visible light irradiation are shown in Figure 3.13. It was observed that the AC can improve the photocatalytic activity of ZnO. In the dark condition, the MB can adsorb on the surface of AC-ZnO and the adsorption capacity of MB was increased as a function of AC loading contents. However, the adsorption capacity of RO did not depend on the AC loading contents as seen in Figure 3.13. As the pH_{pzc} of AC-ZnO composite was about 5.9, it is favor to adsorb MB which is a cationic dye, in the darkness. After illumination, the dyes would be degraded by AC-ZnO composite as shown in Figure 3.13. Rate of dye degradation was increased when the AC loading contents increased from 0.01 g to 0.02 g but the over excess of AC content could depress the degradation rate. From these results, the AC can facilitate visible light absorption leading to enhance the photocatalytic activity of AC-ZnO

3.3. Properties Ag/AC-ZnO composite

3.3.1. Structure and morphology

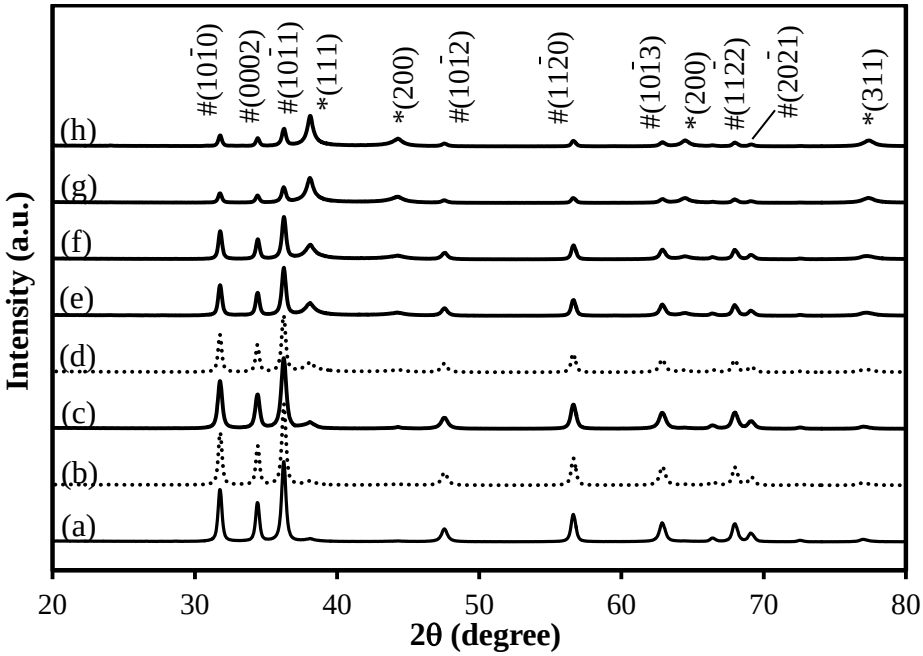

Figure 3.14. XRD patterns of Ag/AC-ZnO at different concentrations of Ag (a) 0.005, (b) 0.01, (c) 0.03, (d) 0.05, (e) 0.07, (f) 0.1, (g) 0.3, and (h) 0.5 M. The peak marked with # can be assigned to ZnO phase and the peak marked with * can be assigned to Ag phase.

Figure 3.14 displays the XRD patterns of Ag/AC-ZnO composite with various Ag loading contents. After data matching with the reference pattern database, it was found that these products consisted of 2 components: ZnO (JCPDS 36-1451) and metallic Ag (JCPDS 04-0783). The metallic Ag deposited on the surface of AC-ZnO occurred through the reduction of the $[Ag(NH_3)_2]^+$ and the intensities of diffracted peaks corresponding to Ag^0 increased with the increment of Ag loadings. Morphologies of AC-ZnO deposited with various Ag contents are shown in Figure 3.15. From Figure 3.4, 3.11 and 3.15, it was clearly to see that Ag/AC-ZnO, AC-ZnO, and ZnO showed the same morphology. In the cause of Ag/AC-ZnO, the presence of Ag on the surface of AC-ZnO had been confirmed by EDX mapping as presented in Figure 3.15 and the results showed that the Ag particles were well dispersed on the surface of agglomerated AC-ZnO composite.

0.01 Ag/AC-ZnO

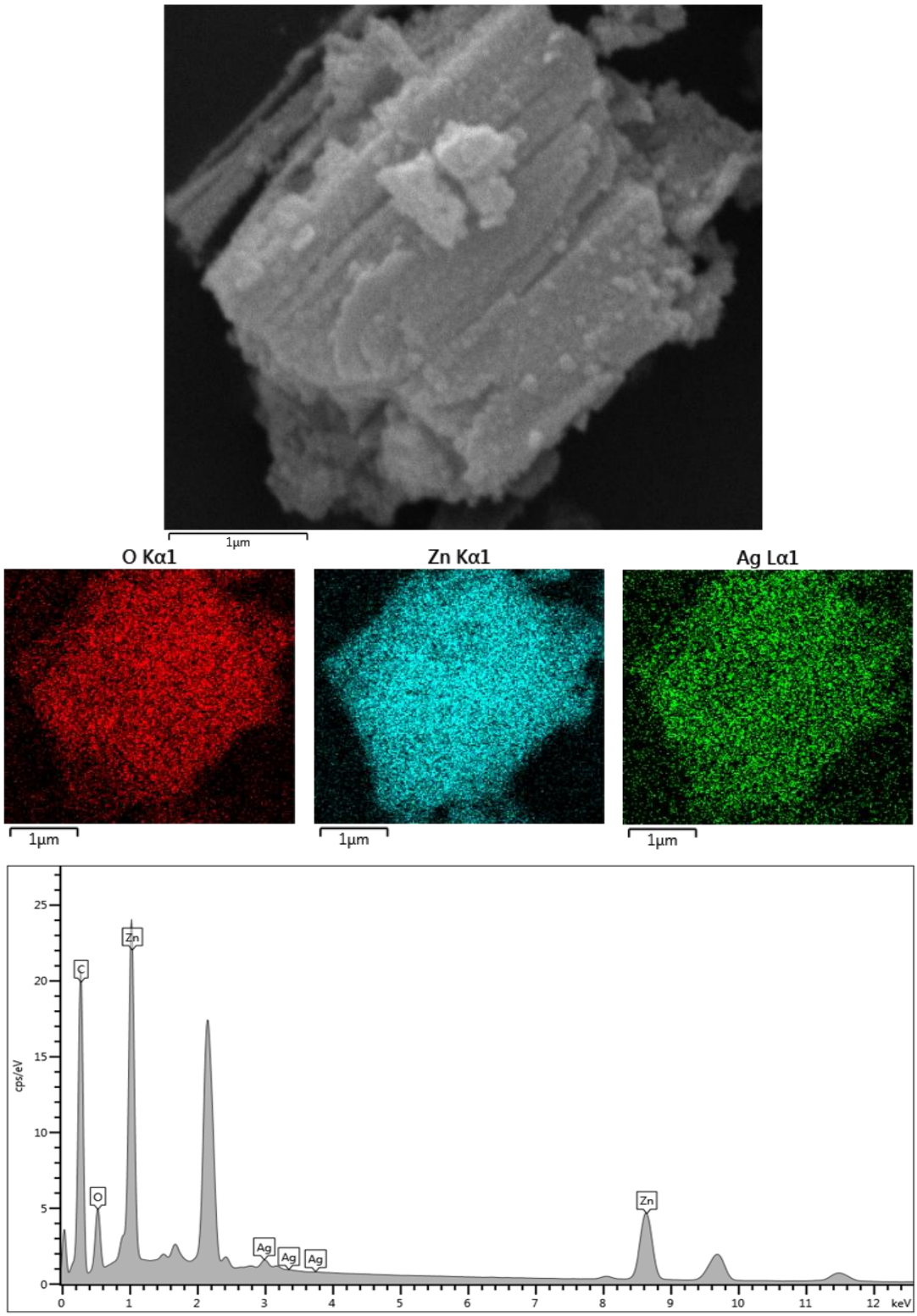

Figure 3.15. SEM images and EDX mapping of Ag/AC-ZnO at different concentrations of Ag.

0.05 Ag/AC-ZnO

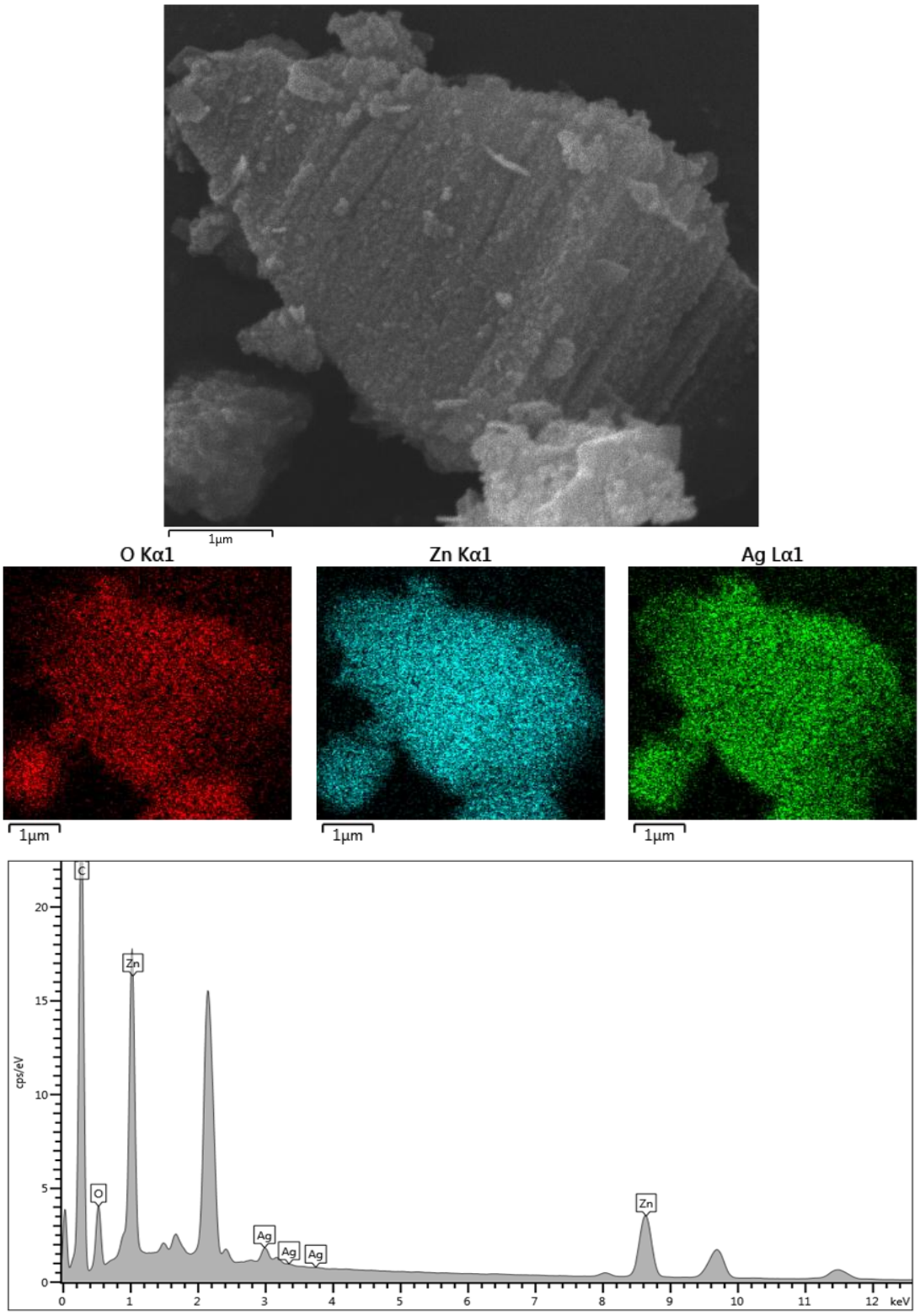

Figure 3.15. (Continued)

0.1 Ag/AC-ZnO

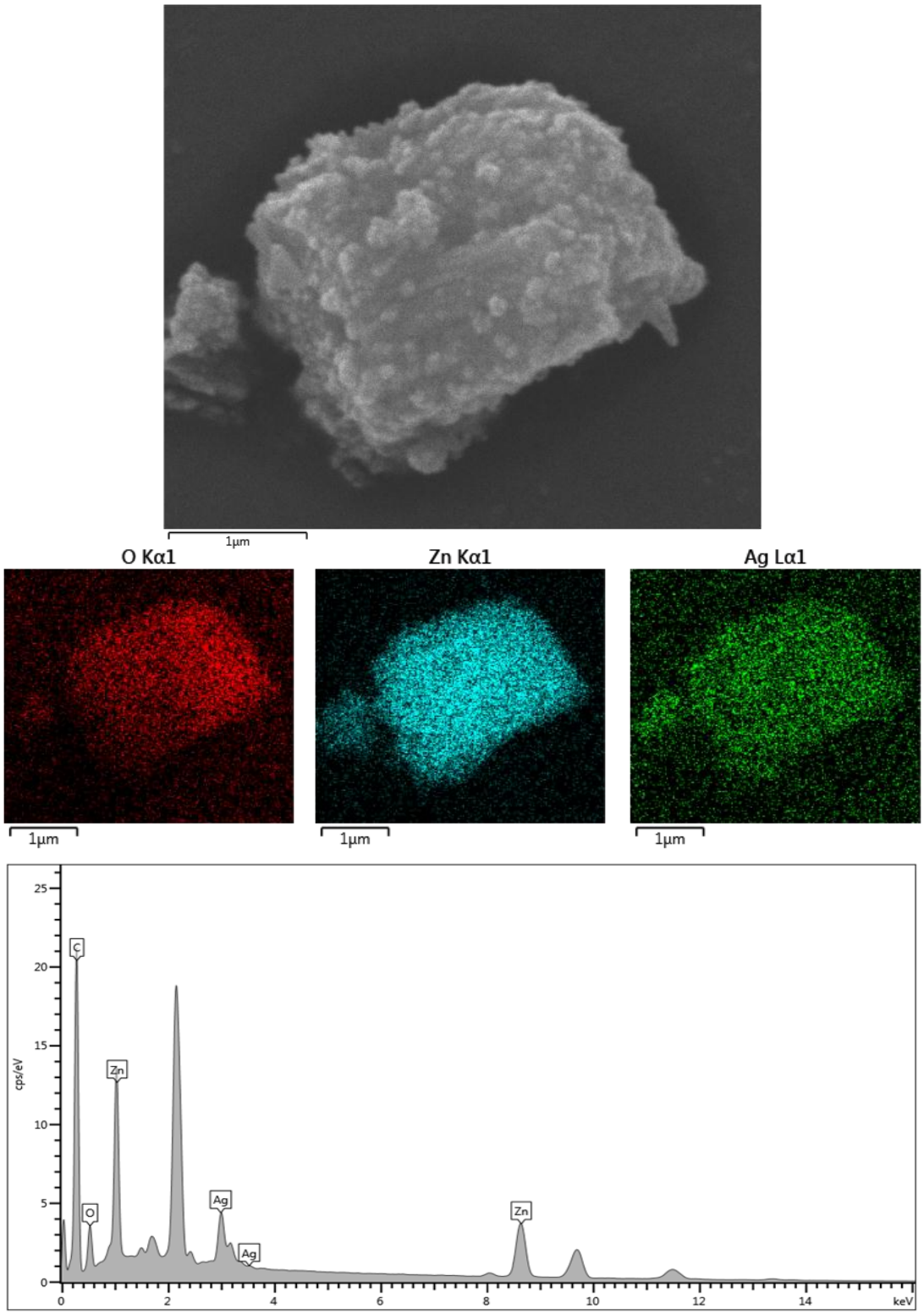

Figure 3.15. (Continued)

0.3 Ag/AC-ZnO

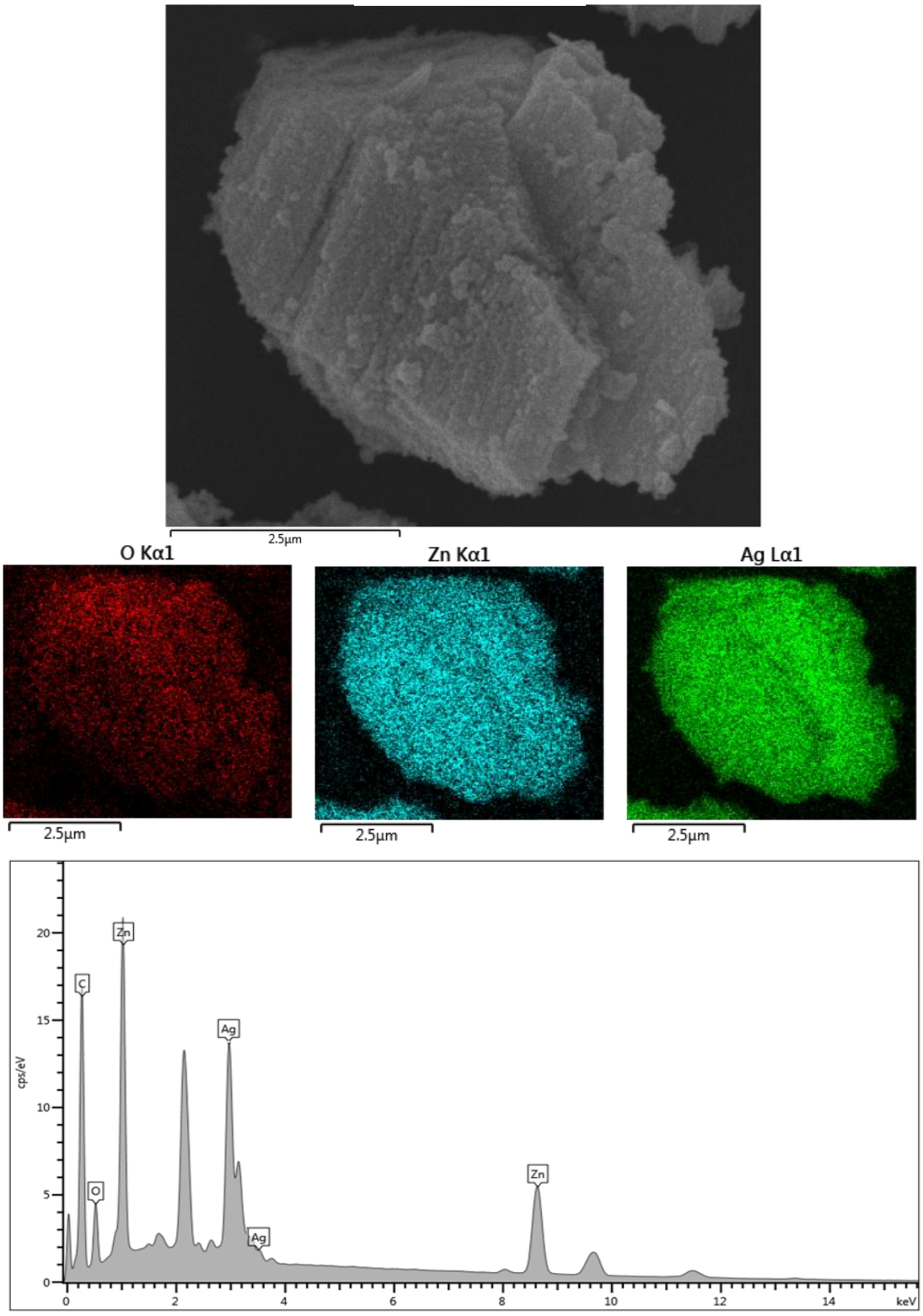

Figure 3.15. (Continued)

3.3.2. Optical properties

The DR spectra of Ag/AC-ZnO composite at different Ag loading contents are shown in Figure 3.16. Comparing with ZnO and AC-ZnO, Ag/AC-ZnO showed the wide broad absorption band in visible region that was attributed to the absorption of Ag on the samples.

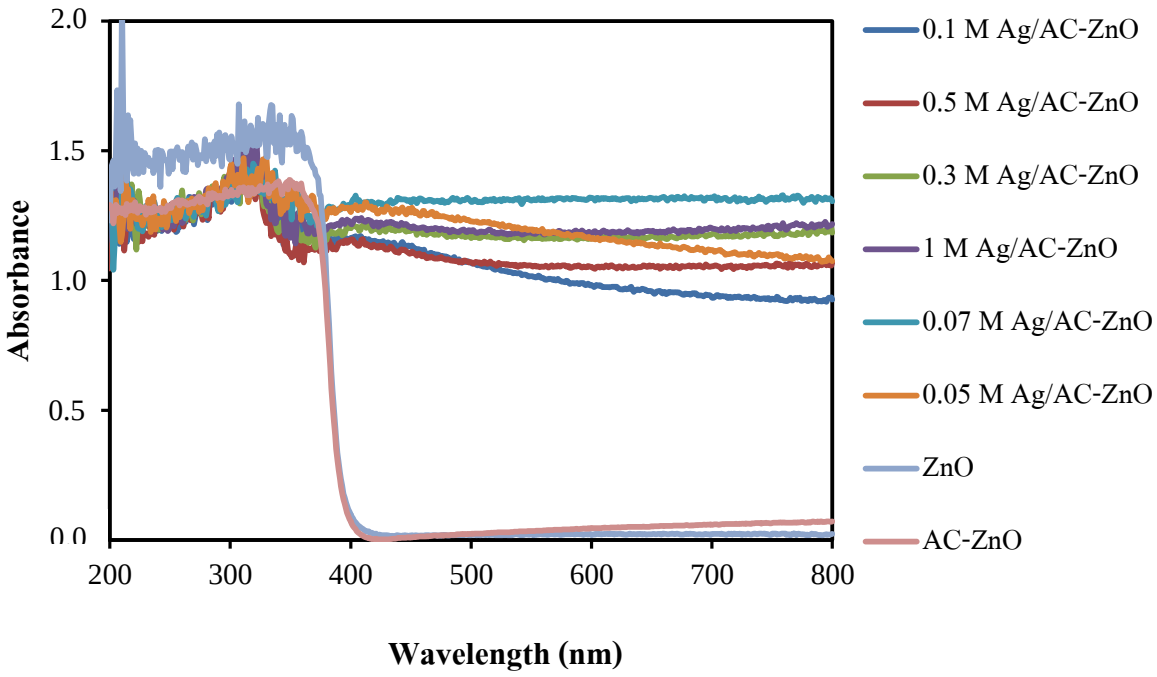

Figure 3.16. The DR spectra for Ag/AC-ZnO composite prepared with different Ag contents.

3.3.3. Photocatalytic Properties of Ag/AC-ZnO composite

The photocatalytic activity of Ag/AC-ZnO powder for degradation of MB and RO are presented in Figure 3.17 and the specific surface areas determined by BET method for all samples are shown in Table 3.1. It was clearly observed that the photocatalytic degradation of dye solution for Ag/AC-ZnO powders did not correlate with their specific surface areas, so their activities should depend on the amount of Ag in photocatalyst. When a concentration of Ag was in the range of 0.05-0.1%, the photocatalytic degradation of MB and RO increased with an increment of the Ag loading content. From Figure 3.16, it was observed that the deposited Ag on the

surface of AC-ZnO composite increased the visible light absorotion ability of the product and this probably enhanced its photocatalytic activity under visible light irradiation. It is well known that the Ag^0 can absorb visible light and generates the photogenerated electrons. These electrons can transfer to ZnO which suppressed the charge recombination during photocatalytic process. Increment of visible light absorption capacity and inhibition of charge recombination can enhance the photocatalytic activity of Ag/AC-ZnO composite. After the Ag content was higher than 0.1%, the photocatalytic activity of Ag/AC-ZnO composite was, however, decreased with an increase in the Ag loading content. This evidence could be attributed to a high coverage of Ag on the surface of AC-ZnO and it probably reduced the surface area of ZnO which reacts with O_2 to from $^{\bullet}O_2^-$ species.

Table 3.1. Specific surface areas evaluated by BET method for ZnO, AC-ZnO, and Ag/AC-ZnO.

Sample	Specific surface area (m^2/g)
ZnO	25.85
AC-ZnO	63.25
0.005Ag/AC-ZnO	29.12
0.01Ag/AC-ZnO	27.08
0.03Ag/AC-ZnO	20.62
0.07Ag/AC-ZnO	16.68
0.1Ag/AC-ZnO	16.37

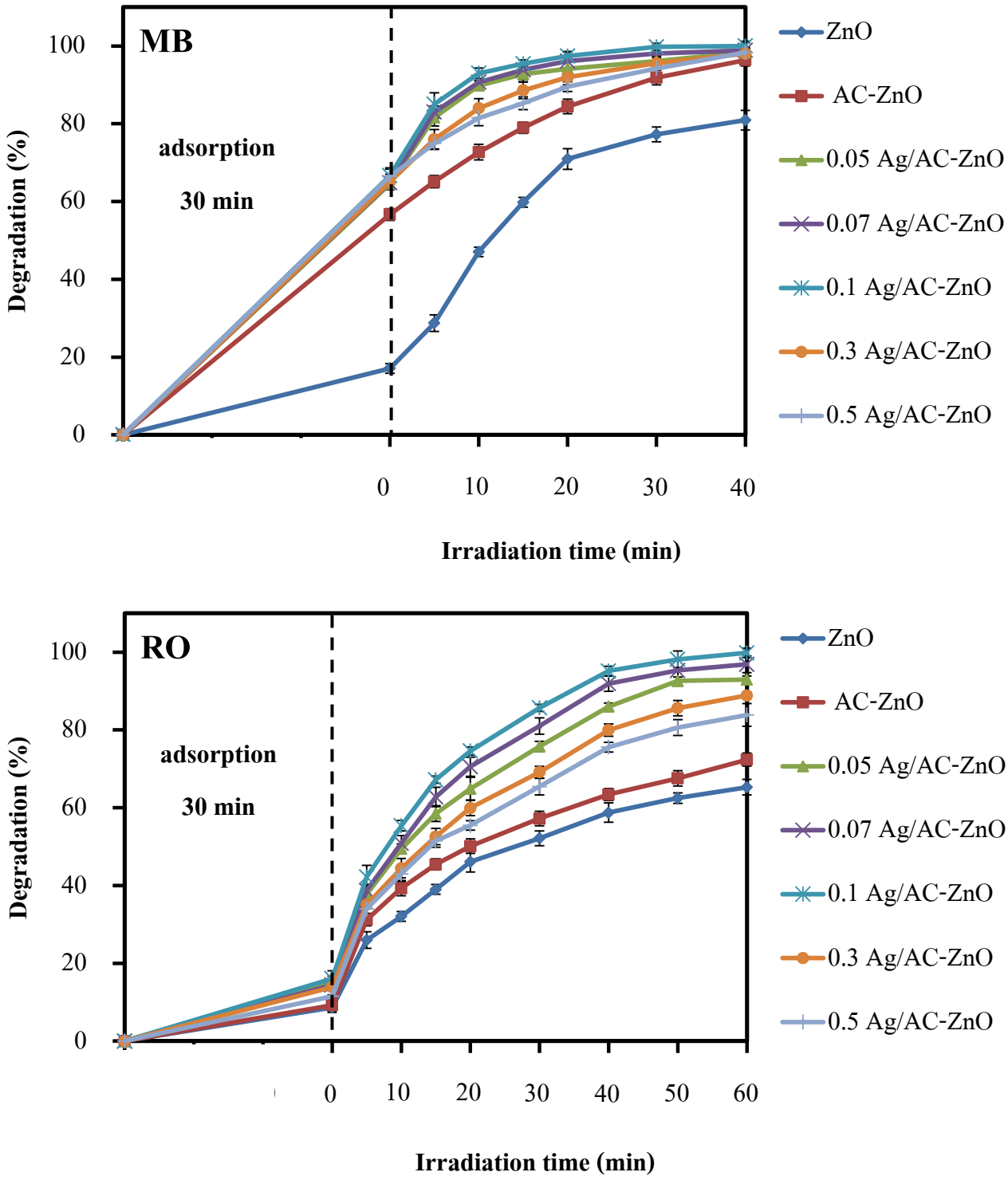

Figure 3.17. The photocatalytic degradation of MB and RO over Ag/AC-ZnO at various Ag loading contents under visible light irradiation.

To evaluate the reactive species involving the photocatalytic process, the suppression in photocatalytic activity using scavengers was achieved in this work and the results are shown in Figure 3.18. After addition of IPA or EDTA-2Na, the

photocatalytic degradation of MB and RO were not significantly different compared with the activity of 0.1Ag/AC-ZnO without scavenger. So, the $^{\bullet}OH$ and h^{+} were not important reactive species in this photocatalytic process. However, the photocatalytic activity of 0.1Ag/AC-ZnO was dramatically decreased when the BQ was added into the dye solution. According to these results, it could be concluded that the $^{\bullet}O_2^{-}$ played the significant role in the degradation of dye under visible light irradiation.

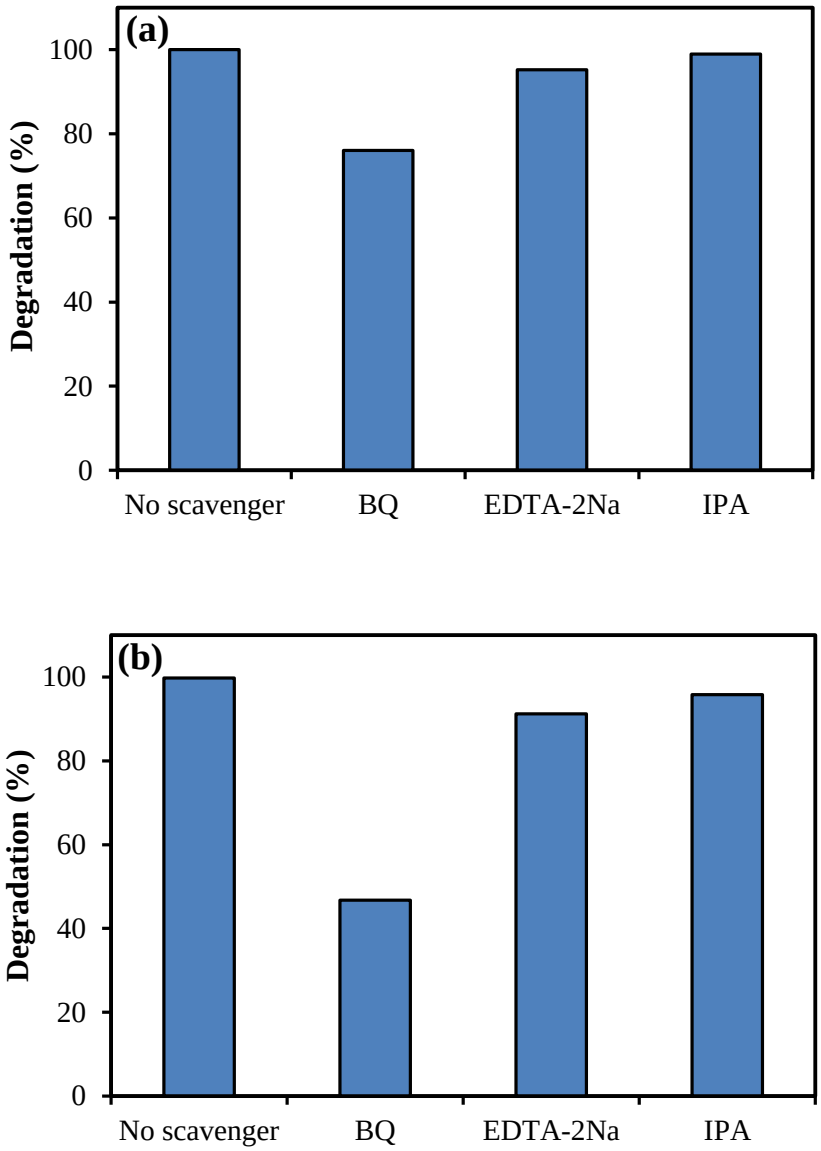

Figure 3.18. Effect of different scavengers on photocatalytic activity of 0.1Ag/AC-ZnO for degradation of (a) MB and (b) RO under visible light irradiation for 60 min.

Influence of pH on photocatalytic activity of prepared 0.1 Ag/AC-ZnO photocatalyst was evaluated by the degradation of MB and RO dyes at pH 3, 5, 7, 9,

and 11. The degradation efficiency for all two dyes under visible light irradiation within 60 min are presented in Figure 3.19.

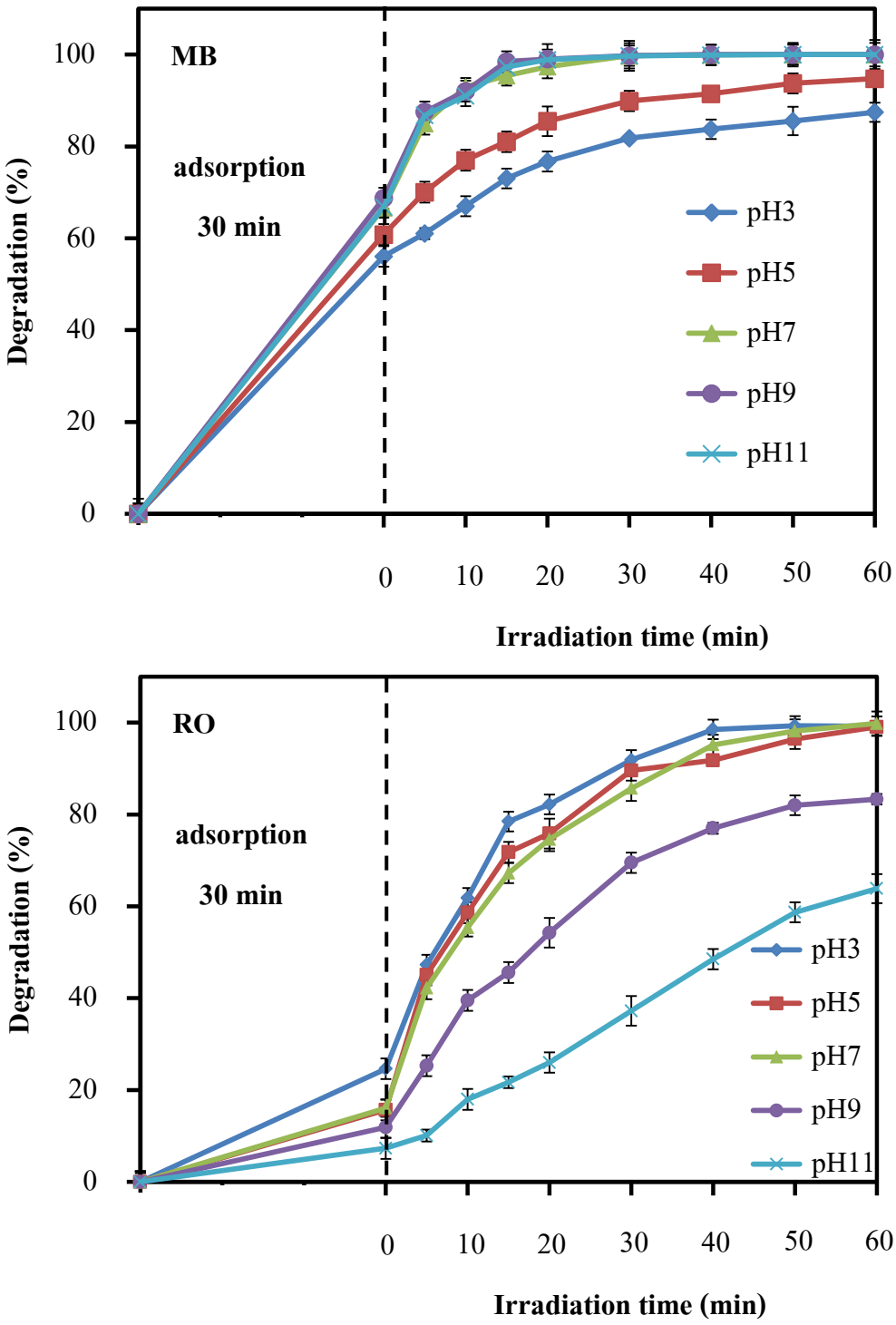

Figure 3.19. The photocatalytic degradation of dye solution for 0.1 Ag/AC-ZnO at various initial pHs under visible irradiation.

When the initial pH was increased, the photocatalytic degradation of MB was increased but this reduced the photocatalytic degradation of RO. This could be explained by an interaction between the dye molecules and the surface of Ag/AC-ZnO. The pH_{pzc} measured by a zeta potential analyzer showed that the pH_{pzc} of 0.1 Ag/AC-ZnO was about 6.5. At pH < pH_{pzc}, the surface of Ag/AC-ZnO has a positive charge and this can adsorb the anionic species. On the other hand, the positive charge of Ag/AC-ZnO repulses the cationic dye and probably increases the photocatalytic activity. The cationic dye was degraded easier than anionic dye at pH > pH_{pzc} because the surface of Ag/AC-ZnO has a negative charge that should attract the cationic dye but repulse the anionic dye.

The reusability and long term stability of the photocatalysts are the key factors for industrial application. The reusability of Ag/AC-ZnO was investigated for degradation of MB and RO under identical reaction condition. The irradiation times for each cycle were 15 min for MB and 60 min for RO.

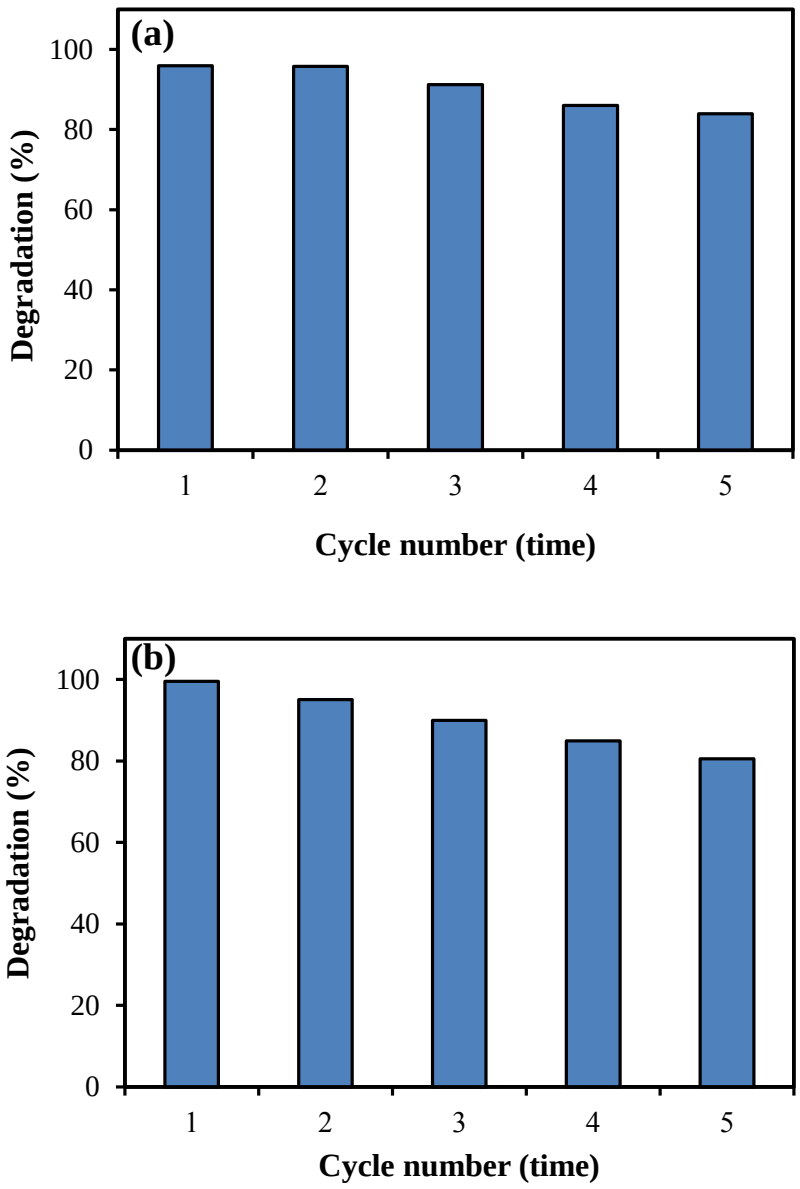

Figure 3.20. Reusability of 0.1Ag/AC-ZnO to degrade (a) MB and (b) RO under visible light irradiation.

After each cycling experiment, the photocatalyst was separated and washed with a large amount of D.I. water. As shown in Figure 3.20, the photostability of 0.1Ag/AC-ZnO composite was verified by five recycling test for degradation of MB and RO under visible light irradiation. It was clearly observed that the photocatalytic dye degradation decreased with increasing recycling times. After the fifth cycle, the photocatalytic activity was more than 80% implied that Ag/AC/ZnO showed good stability and sustainability.

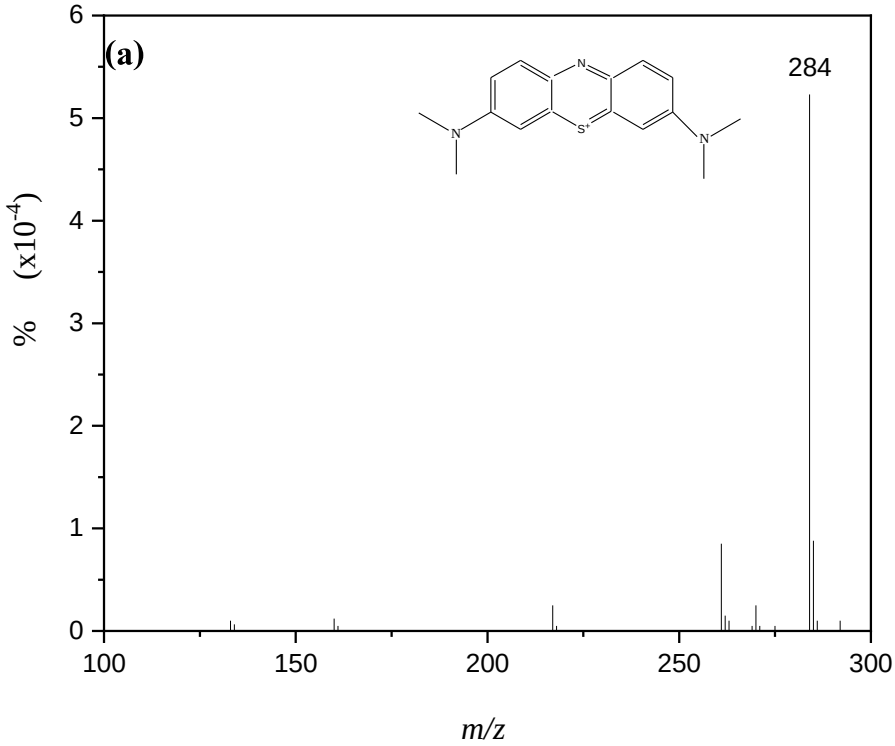

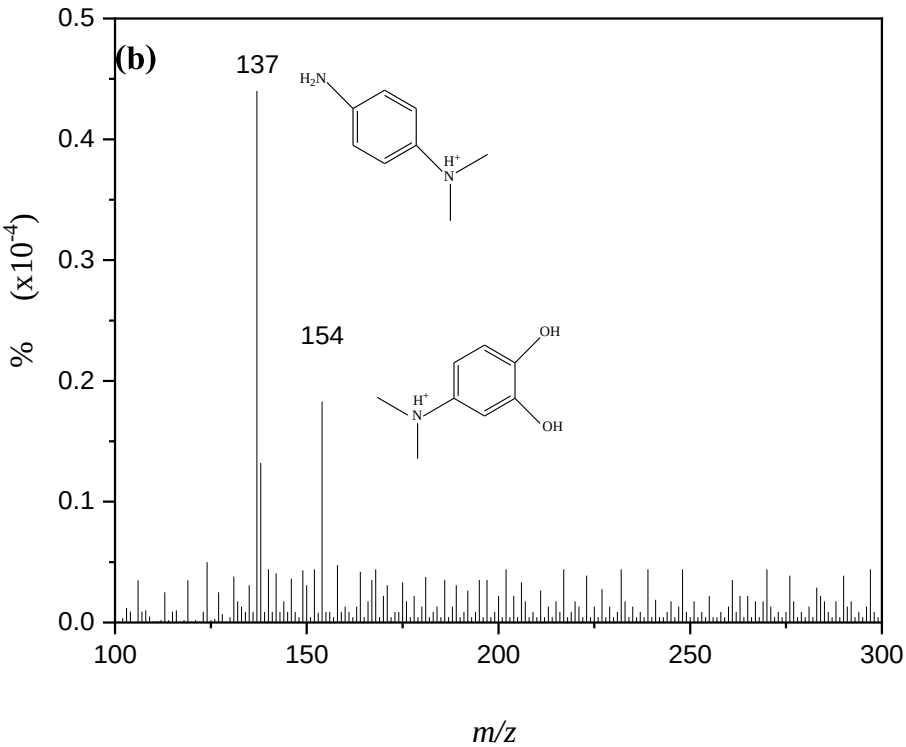

Figure 3.21. ESI^{+} mass spectra of (a) initial MB and (b) MB after irradiation for 40 min and ESI^{-} mass spectra of (c) initial RO and (e) RO after irradiation for 60 min.

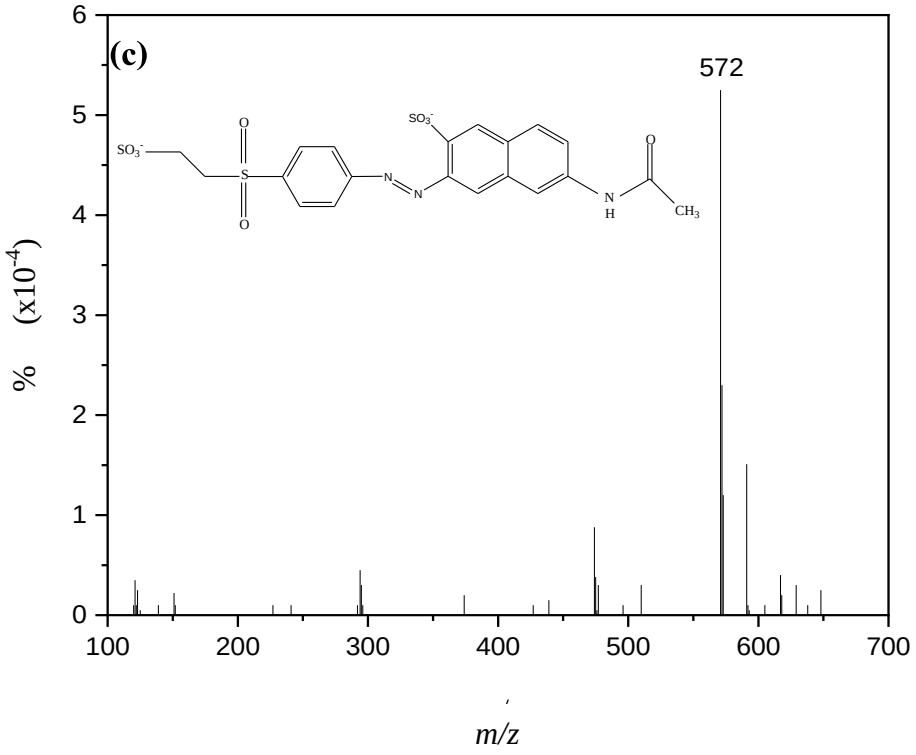

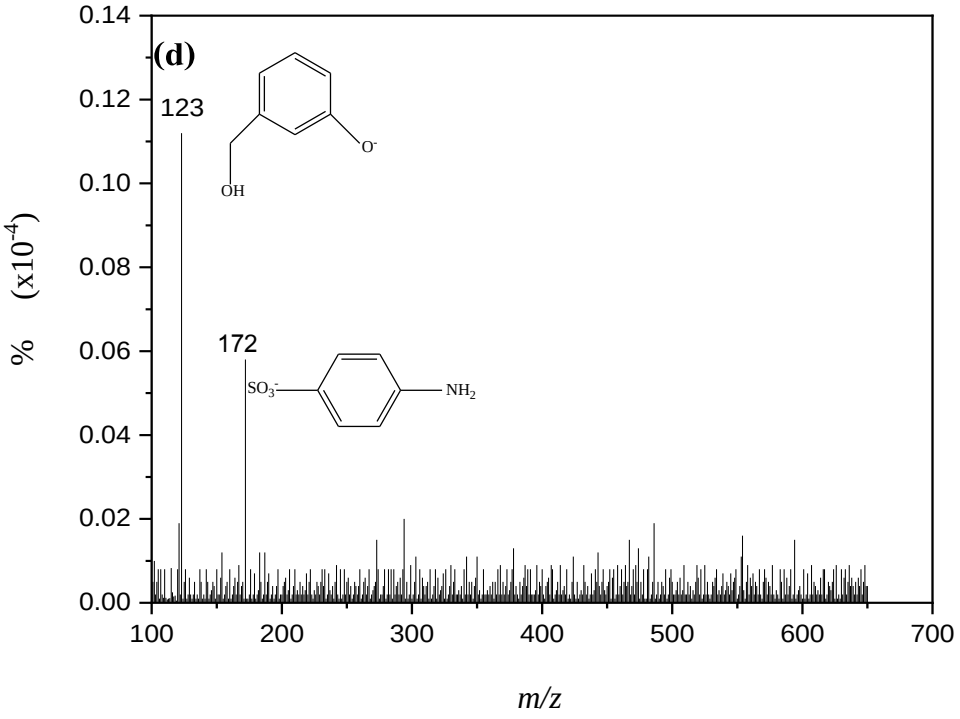

Figure 3.21. (Continued)

To confirm the degradation of dye, the ESI mass spectrometry, which was operated in positive mode for MB and negative mode for RO, was used to identify the species before and after photocatalysis and the results are shown in Figure 3.21. The MB solution before photocatalysis showed the parent mass at *m/z* = 284 corresponding to $[MB\text{-}Cl]^+$ as presented in Figure 3.21 (a). After irradiation for 40 min with Ag/AC-ZnO, this peak was not observed but there were two main peaks at *m/z* = 137 and 154 as seen in Figure 3.21 (b). The peak at *m/z* = 571 as shown in Figure 3.21 (c) was assigned to $[RO\text{-}2Na]^{2-}$ species and it was not detectable after irradiation for 60 min. Figure 3.21 (e) displays the ESI^- mass spectrum of RO solution after irradiation for 60 min and this result indicated that the RO molecules could be degraded to the species which have *m/z* = 123 and 172. From above results, it probably confirmed that Ag/AC-ZnO can degrade MB and RO molecules under visible light irradiation.

According to results of mass spectrometry as presented in Figure 3.21, it can be implied that most of dye molecules were degraded and probably converted to CO_2 that lost from the system. However, after photocatalysis, many small molecules were detectable. To compare the toxicity of parent dyes and the degraded product, an in vitro cytotoxicity test for dye solution before and after irradiation was studied through the relative viability of L-929 mouse fibroblast cells after exposure to these solutions using MTT assay. Table 3.2 presents the cell viability after incubation for 72 h with dye solution before and after photocatalysis. It observes that the dye solution after photocatalysis were less cytotoxic than their initial solution.

Table 3.2. Cell viability of L-929 cells in dye solution before and after photocatalysis.

Solution	Viability (%)	
	MB	RO
Before photocatalysis	17.28 ± 2.44	41.71 ± 2.48
After photocatalysis (40 min for MB and 60 min for RO)	66.14 ± 2.66	77.58 ± 1.55

Reverse osmosis water = 100% survival

3.3.4. Bisphenol A

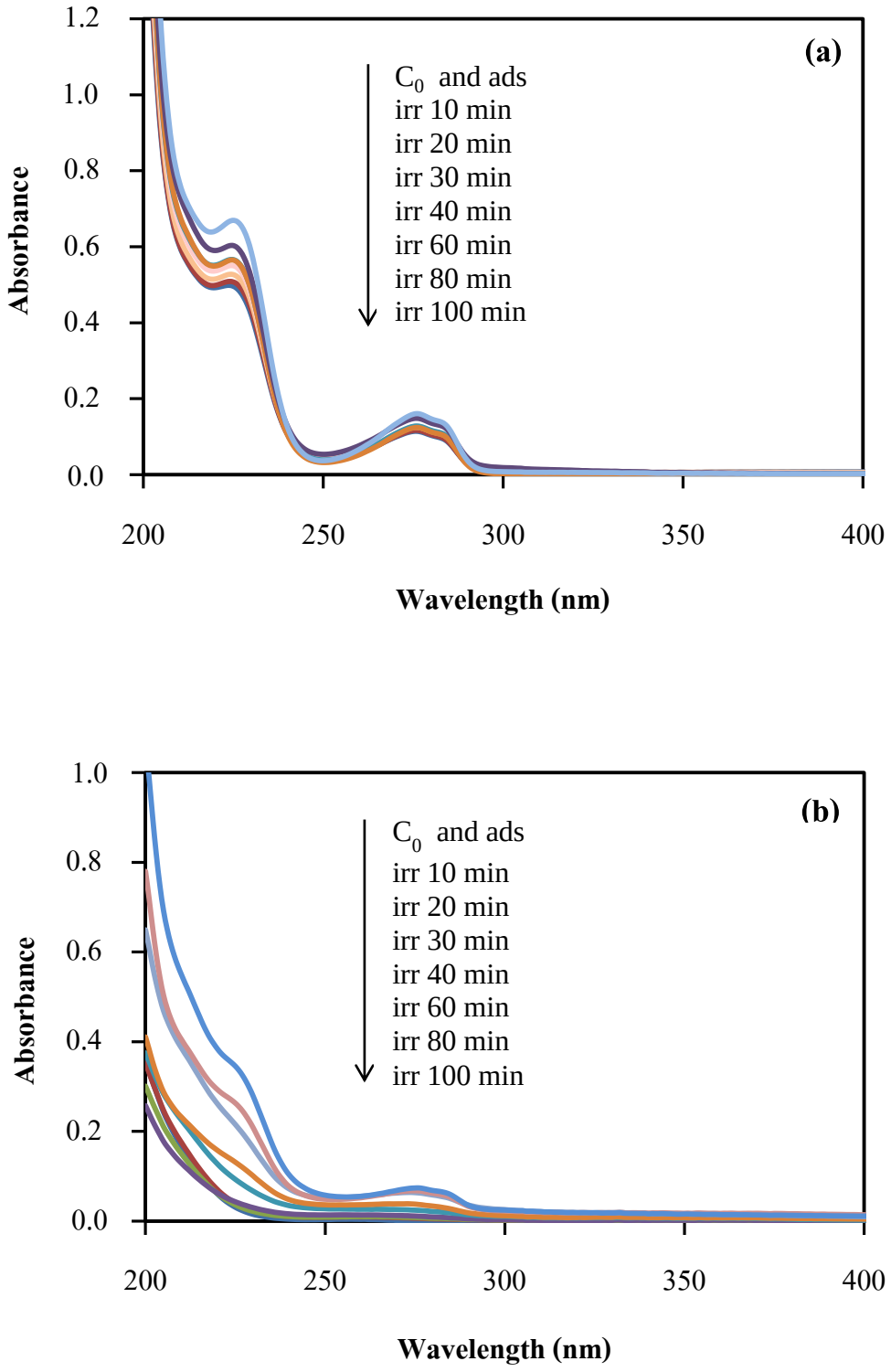

Figure 3.22. Chronological change in absorption spectra of BPA (a) without H_2O_2 and (b) with H_2O_2 using 0.03Ag/AC-ZnO as photocatalyst under visible light irradiation.

Figure 3.22 (a) shows the absorption spectra of BPA with 0.03Ag/AC-ZnO as a function of irradiation time. As the absorbance of BPA solution before and after photocatalysis were not significantly different, it could be concluded that Ag/AC-ZnO cannot degraded BPA molecules at this condition. Thus, the H_2O_2 was added into the BPA solution in order to facilitate the rate of reactive species production. After addition of H_2O_2, the absorbance of BPA decreased with increasing an irradiation times as shown in Figure 3.22 (b) implying that H_2O_2 was important additive to assist photocatalytic degradation of BPA when using Ag/AC-ZnO as photocatalyst under visible light irradiation.

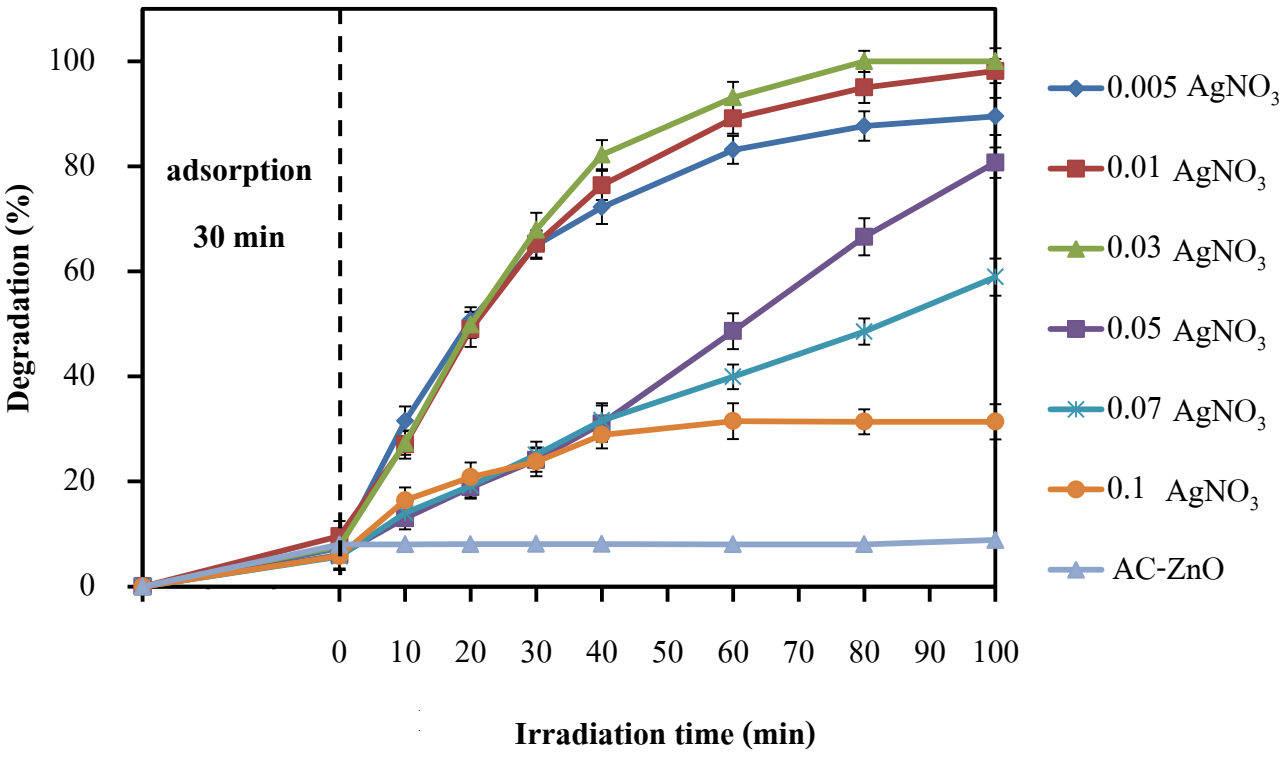

Figure 3.23. The photocatalytic degradation of BPA in the presence of H_2O_2 over Ag/AC-ZnO at various Ag loading under visible light irradiation.

The photocatalytic degradation of BPA with H_2O_2 in the presence of Ag/AC-ZnO at various amounts of Ag is illustrated in Figure 3.22. It was clearly observed that the photocatalytic activity can be divided into 2 groups. At 0.005-0.03Ag/AC-ZnO, their photocatalytic activities increased with the increment of Ag loading contents and the 0.03 Ag/AC-ZnO showed the best activity. After this point, the photocatalytic activity decreased as seen in Figure 3.23. This evidence could be

attributed to the high coverage of Ag on the surface of AC-ZnO. Actually, the photogenerated electrons of metallic Ag would transfer to the conduction band of AC-ZnO and these electrons react with O_2 to form $^{\bullet}O_2^{-}$. So, the specific surface area of AC-ZnO could be reduced at high Ag loading content.

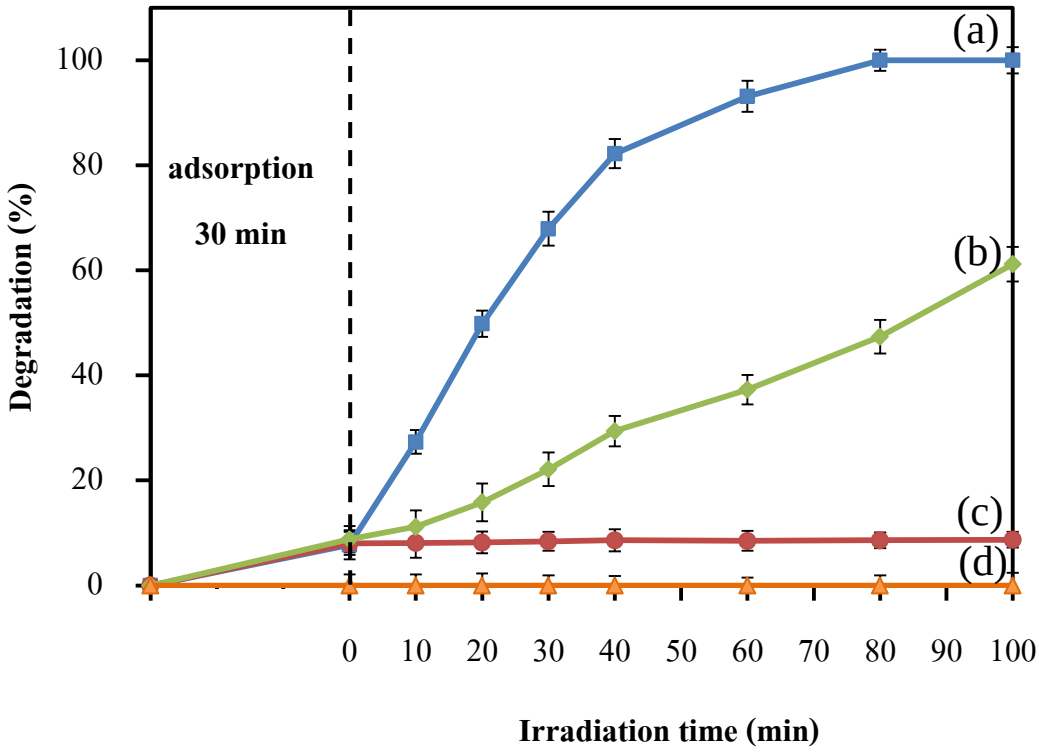

Figure 3.24. The photocatalytic degradation of BPA solution using 0.03 Ag/AC-ZnO as photocatalyst: (a) with H_2O_2 under visible light irradiation, (b) with air bubble under visible light irradiation, (c) with H_2O_2 in the dark condition, and (d) with H_2O_2 under visible light irradiation (no photocatalyst).

Indeed, when the H_2O_2 molecules contact with metallic Ag, the O_2 gas would be produced by the following reaction:

$$2H_2O_2 + Ag(s) \longrightarrow H_2O(l) + O_2(g) + Ag(s) \quad (3.2)$$

To study the effect of this reaction on photocatalytic degradation of BPA, the BPA solution with H_2O_2 and 0.03 Ag/AC-ZnO was stirred in the dark. As the result presented in Figure 3.24 (c), it could be concluded that this reaction did not degrade the BPA molecules. On the other hand, the 0.03 Ag/AC-ZnO can degrade the BPA molecules when this solution was exposured to visible light as seen in Figure 3.24 (a).

From Eq(3.2), the decomposition of H_2O_2 would generate O_2 that probably influence the photocatalytic activity of 0.03 Ag/AC-ZnO. To confirm this hypothesis, the H_2O_2 as a source of O_2 was replaced by O_2 blowing. At this condition, the 0.03 Ag/AC-ZnO showed the photocatalytic degradation of BPA without addition of H_2O_2 as illustrated in Figure 3.24(b). For this evidence, it could be concluded that the dissolving O_2 is an important factor to enhance the photocatalytic degradation of BPA in this system.

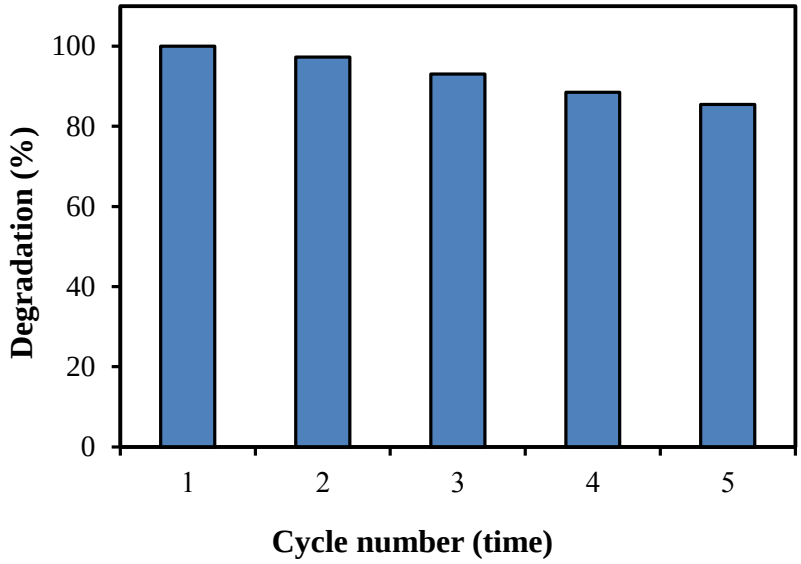

Figure 3.25. Reusability of 0.03 Ag/AC-ZnO for degradation of BPA in the presence of H_2O_2 under visible light irradiation for 100 min.

Figure 3.25 displays the photocatalytic degradation of BPA for five run. It was observed that the photocatalytic activity of 0.03 Ag/AC-ZnO decreased with increasing the number of recycle. However, the photocatalytic degradation of BPA still remained more than 85% implying that this photocatalyst was relatively stable under visible light irradiation.

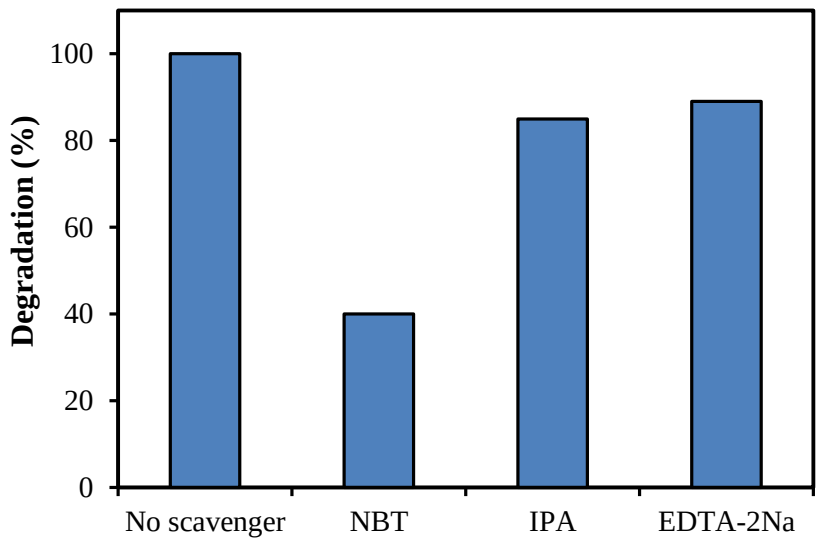

Figure 3.26. Photocatalytic degradation of BPA with H_2O_2 and 0.03 Ag/AC-ZnO in the absence of scavenger and in the presence of NBT, IPA, and EDTA-2Na under visible light irradiation for 100 min.

In this work, the suppression in photocatalytic activity technique using scavengers was achieved in order to investigate the important reactive species involving the photocatalytic degradation. The results for this study are shown in Figure 3.26. When the IPA or EDTA-2Na was added into BPA solution, the photocatalytic degradation of BPA was not significantly different compared with the activity of 0.03 Ag/AC-ZnO without scavenger. It could be said that the $^{\bullet}OH$ and h^+ were not the main reactive species to degrade BPA. However, the photocatalytic activity of 0.03 Ag/AC-ZnO dramatically decreased when the NBT was added into the dye solution. According to these results, it could be concluded that the $^{\bullet}O_2^-$ played the significant role in the degradation of dye under visible light irradiation.

To confirm the degradation of BPA, the degraded species after photocatalysis were identified by ESI mass spectrometry operated in negative mode and the results are presented in Figure 3.27. Before photocatalysis, the BPA showed a parent peak at m/z = 227.2 as presented in Figure 3.27(a) corresponding to $[M-H]^-$ ion. After irradiation for 120 min, there was no detectable peak in the range of *m/z* = 100-300 as seen in Figure 3.27(b). It implied that the BPA molecules probably degraded during photocatalytic processes to small molecules with their masses less than 100.

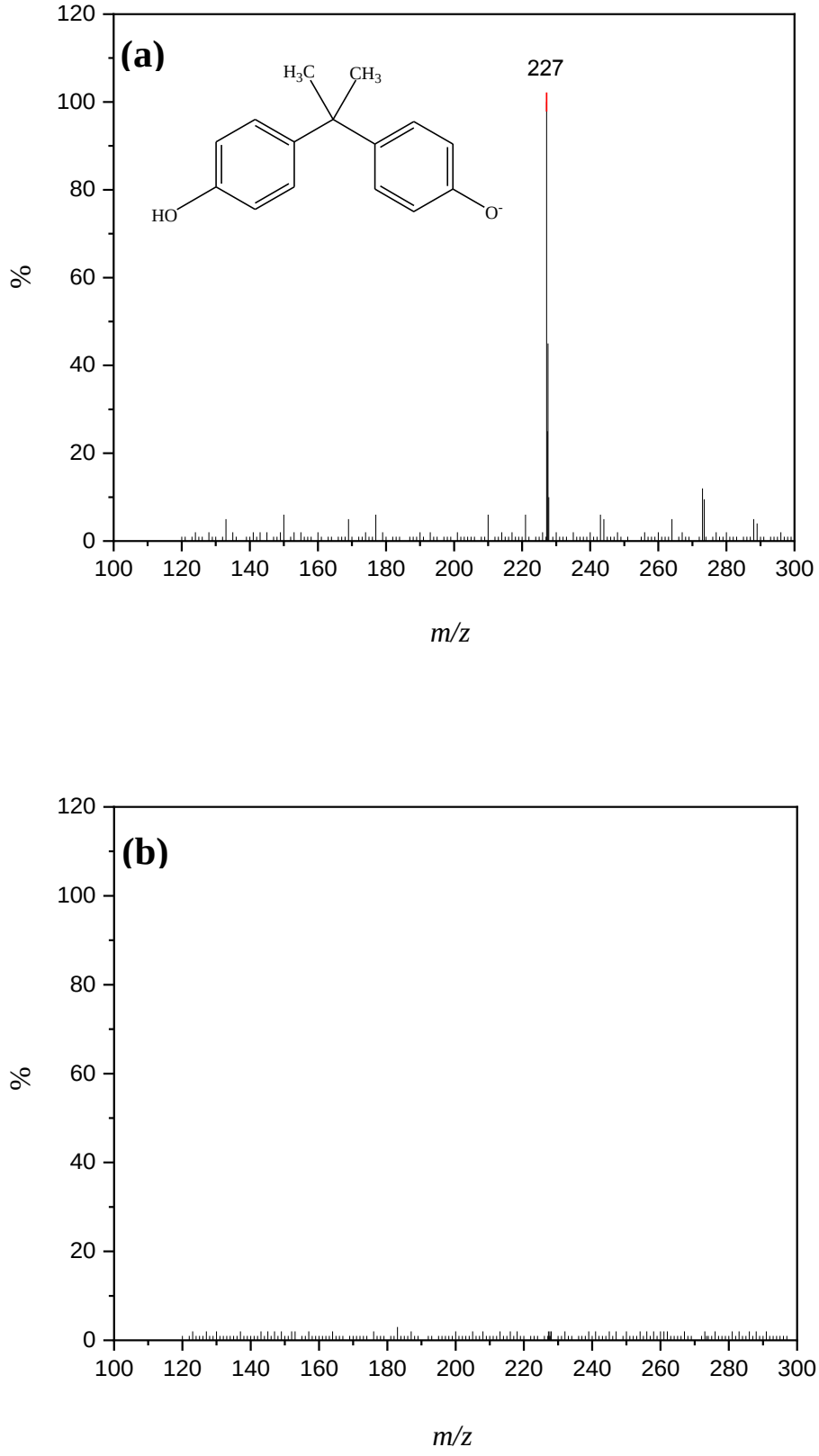

Figure 3.27. ESI$^-$ mass spectra of (a) initial BPA and (b) BPA after irradiation for 120 min

To compare the toxicity of BPA and their degraded products, an in vitro cytotoxicity test for BPA solution before and after irradiation was studied through the relative viability of L-929 mouse fibroblast cells after exposure to these solutions using MTT assay. Table 3.3 presents the cell viability after incubation for 72 h with BPA solution before and after photocatalysis. It was observed that the BPA solutions after photocatalysis were less cytotoxic than their initial solutions.

Table 3.3. Cell viability of L-929 cells in BPA solutions before and after photocatalysis.

Solution	Viability (%)
BPA solution before photocatalysis	67.553 $\pm$ 5.138
BPA solution after photocatalysis (120 min irradiation)	99.640 $\pm$ 5.285

Reverse osmosis water = 100% survival

CHAPTER 4

CONCLUSIONS

After the mixture between $Zn(NO_3)_2.6H_2O$ and $X_2C_2O_4$ (X = H, Na, NH_4) solutions was heated at 80 ^oC for 1 h, the resulting product was assigned to $ZnC_2O_4.2H_2O$ as the intermediate compound. Compared with $Na_2C_2O_4$ and $(NH_4)_2C_2O_4$, the $ZnC_2O_4.2H_2O$ prepared from $H_2C_2O_4$ exhibited the largest particle that was broken up into smaller agglomerated ZnO nanoparticles after calcination at 500 ^oC for 1 h and subsequently produced a ZnO with a high specific surface area. Thus, the ZnO prepared from $H_2C_2O_4$ showed the best activity for degradation of methylene blue (MB) and reactive orange (RO) solutions under blacklight irradiation. As the E_g of this ZnO was 3.219 eV, it demonstrated a low efficiency of dye degradation under visible light irradiation. In order to improve the ability of visible light absorption, activated carbon (AC) and metallic silver (Ag) were added into ZnO particles. Ag/AC-ZnO exhibited higher photocatalytic activity than pure ZnO, AC-ZnO, and Ag/ZnO under visible light irradiation. From experimental results, 0.1Ag/AC-ZnO showed the highest photocatalytic degradation of MB and RO solution while the maximum degradation of bisphenol A (BPA) was observed for 0.03Ag/AC-ZnO in the presence of H_2O_2 as an additive. The mechanism of photocatalytic degradation for Ag/AC-ZnO under visible light irradiation could be proposed as follows:

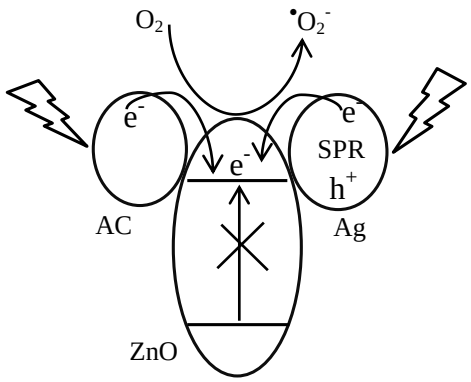

After photocatalysis, the MB, RO and BPA were decomposed to low molecular weight products confirmed by mass spectrometry and these degraded products exhibited less toxic to normal L-929 cells than their initial solutions.

REFERENCES

Hsu, M.-H., & Chang, C.-J. (2014). Ag-doped ZnO nanorods coated metal wire meshes as hierarchical photocatalysts with high visible-light driven photoactivity and photostability. *Journal of Hazardous Materials*, *278*, 444–453.

Baitha, P. Kr., Pal, P. P., & Manam, J. (2014). Dosimetric sensing and optical properties of ZnO–SnO_2 nanocomposites synthesized by co-precipitation method. *Nuclear Instruments and Methods in Physics Research Section A: Accelerators, Spectrometers, Detectors and Associated Equipment*, *745*, 91–98.

Bouzid, H., Faisal, M., Harraz, F. A., Al-Sayari, S. A., & Ismail, A. A. (2015). Synthesis of mesoporous Ag/ZnO nanocrystals with enhanced photocatalytic activity. *Catalysis Today*, *252*, 20–26.

Bozetine, H., Wang, Q., Barras, A., Li, M., Hadjersi, T., Szunerits, S., & Boukherroub, R. (2016). Green chemistry approach for the synthesis of ZnO–carbon dots nanocomposites with good photocatalytic properties under visible light. *Journal of Colloid and Interface Science*, *465*, 286–294.

Chaudhary, D., Singh, S., Vankar, V. D., & Khare, N. (2018). ZnO nanoparticles decorated multi-walled carbon nanotubes for enhanced photocatalytic and photoelectrochemical water splitting. *Journal of Photochemistry and Photobiology A: Chemistry*, *351*, 154–161.

Çolak, H., Karaköse, E., & Derin, Y. (2017). Properties of ZnO nanostructures produced by mechanochemical-solid state combustion method using different precursors. *Materials Chemistry and Physics*, *193*, 427–437.

Daou, I., Zegaoui, O., & Elghazouani, A. (2017). Physicochemical and photocatalytic properties of the ZnO particles synthesized by two different methods using three different precursors. *Comptes Rendus Chimie*, *20*(1), 47–54.

Dong, Y., Jiao, Y., Jiang, B., & Tian, C. (2017). Commercial ZnO and its hybrid with Ag nanoparticles: Photocatalytic performance and relationship with structure. *Chemical Physics Letters*, *679*, 137–145.

Han, Z., Ren, L., Cui, Z., Chen, C., Pan, H., & Chen, J. (2012). Ag/ZnO flower heterostructures as a visible-light driven photocatalyst via surface plasmon resonance. *Applied Catalysis B: Environmental*, *126*, 298–305.

Hsu, M.-H., & Chang, C.-J. (2014). Ag-doped ZnO nanorods coated metal wire meshes as hierarchical photocatalysts with high visible-light driven photoactivity and photostability. *Journal of Hazardous Materials*, *278*, 444–453.

Jasso-Salcedo, A. B., Palestino, G., & Escobar-Barrios, V. A. (2014). Effect of Ag, pH, and time on the preparation of Ag-functionalized zinc oxide nanoagglomerates as photocatalysts. *Journal of Catalysis*, *318*, 170–178.

Jia, Z., Ren, D., Xu, L., & Zhu, R. (2012). Preparation, characterization and photocatalytic activity of porous zinc oxide superstructure. *Materials Science in Semiconductor Processing*, *15*(3), 270–276.

Kahouli, M., Barhoumi, A., Bouzid, A., Al-Hajry, A., & Guermazi, S. (2015). Structural and optical properties of ZnO nanoparticles prepared by direct precipitation method. *Superlattices and Microstructures*, *85*, 7–23.

Kanchana, S., Chithra, M. J., Ernest, S., & Pushpanathan, K. (2016). Violet emission from Fe doped ZnO nanoparticles synthesized by precipitation method. *Journal of Luminescence*, *176*, 6–14.

Khademalrasool, M., Farbod, M., & Iraji zad, A. (2016). Preparation of ZnO nanoparticles/Ag nanowires nanocomposites as plasmonic photocatalysts and investigation of the effect of concentration and diameter size of Ag nanowires on their photocatalytic performance. *Journal of Alloys and Compounds*, *664*, 707–714.

Kong, X., Zhang, X., & Chen, J. (2015). Highly active and selective CoCu/ZnO catalysts prepared by mild oxalic acid co-precipitation method in dimethyl oxalate hydrogenation. *Catalysis Communications*, *65*, 46–50.

Kumar, Rajesh, Umar, Ahmad, Kumar, Girish, & Nalwa, H. S. (2017). Antimicrobial properties of ZnO nanomaterials: A review. *Ceramics International*, *43*(5), 3940–3961.

Lanje, A. S., Sharma, S. J., Ningthoujam, R. S., Ahn, J.-S., & Pode, R. B. (2013). Low temperature dielectric studies of zinc oxide (ZnO) nanoparticles prepared by precipitation method. *Advanced Powder Technology*, *24*(1), 331–335.

Lee, K. S., Park, C. W., & Kim, J.-D. (2017). Electrochemical properties and characterization of various ZnO structures using a precipitation method. *Colloids and Surfaces A: Physicochemical and Engineering Aspects*, *512*, 87–92.

Lesmana, D., & Wu, H.-S. (2014). Modified oxalic acid co-precipitation method for preparing Cu/ZnO/Al_2O_3/Cr_2O_3/CeO_2 catalysts for the OR (oxidative reforming) of M (methanol) to produce H2 (hydrogen) gas. *Energy*, *69*, 769–777.

Li, L., Yang, H., Yu, J., Chen, Y., Ma, J., Zhang, J., … Gao, F. (2009). Controllable growth of ZnO nanowires with different aspect ratios and microstructures and their photoluminescence and photosensitive properties. *Journal of Crystal Growth*, *311*(17), 4199–4206.

Liu, Y., Xu, C., Zhu, Z., Lu, J., Manohari, A. G., & Shi, Z. (2018). Self-assembled ZnO/Ag hollow spheres for effective photocatalysis and bacteriostasis. *Materials Research Bulletin*, *98*, 64–69.

Moradi, M., Haghighi, M., & Allahyari, S. (2017). Precipitation dispersion of Ag–ZnO nanocatalyst over functionalized multiwall carbon nanotube used in degradation of Acid Orange from wastewater. *Process Safety and Environmental Protection*, *107*, 414–427.

Muñoz-Fernandez, L., Sierra-Fernandez, A., Flores-Carrasco, G., Milošević, O., & Rabanal, M. E. (2017). Solvothermal synthesis of Ag/ZnO micro/nanostructures with different precursors for advanced photocatalytic applications. *Advanced Powder Technology*, *28*(1), 83–92.

Muthirulan, P., Meenakshisundararam, M., & Kannan, N. (2013). Beneficial role of ZnO photocatalyst supported with porous activated carbon for the mineralization of alizarin cyanin green dye in aqueous solution. *Journal of Advanced Research*, *4*(6), 479–484.

Qi, K., Cheng, B., Yu, J., & Ho, W. (2017). Review on the improvement of the photocatalytic and antibacterial activities of ZnO. *Journal of Alloys and Compounds*, *727*, 792–820.

Ong, C. B., Ng, L. Y., & Mohammad, A. W. (2018). A review of ZnO nanoparticles as solar photocatalysts: Synthesis, mechanisms and applications. *Renewable and Sustainable Energy Reviews*, *81*, 536–551.

Pan, L., Xu, M., & Zhang, Z. (2010). A general synthesis and electrocatalytic activity of low-dimensional MO and M–Co (MCu, Ni, Zn and Cd) composite oxides. *Materials Chemistry and Physics*, *123*(1), 293–299.

Pant, B., Park, M., Kim, H.-Y., & Park, S.-J. (2016). Ag-ZnO photocatalyst anchored on carbon nanofibers: Synthesis, characterization, and photocatalytic activities. *Synthetic Metals*, *220*, 533–537.

Pulido Melián, E., González Díaz, O., Doña Rodríguez, J. M., Colón, G., Araña, J., Herrera Melián, J., … Peña, J. P. (2009). ZnO activation by using activated carbon as a support: Characterisation and photoreactivity. *Applied Catalysis A: General*, *364*(1), 174–181.

Rafaie, H. A., Nor, R. M., Azmina, M. S., Ramli, N. I. T., & Mohamed, R. (2017). Decoration of ZnO microstructures with Ag nanoparticles enhanced the catalytic photodegradation of methylene blue dye. *Journal of Environmental Chemical Engineering*, *5*(4), 3963–3972.

Raj, K. P., & Sadayandi, K. (2016). Effect of temperature on structural, optical and photoluminescence studies on ZnO nanoparticles synthesized by the standard co-precipitation method. *Physica B: Condensed Matter*, *487*, 1–7.

Raizada, P., Singh, P., Kumar, A., Sharma, G., Pare, B., Jonnalagadda, S. B., & Thakur, P. (2014). Solar photocatalytic activity of nano-ZnO supported on activated carbon or brick grain particles: Role of adsorption in dye degradation. *Applied Catalysis A: General*, *486*, 159–169.

Raoufi, D. (2013). Synthesis and microstructural properties of ZnO nanoparticles prepared by precipitation method. *Renewable Energy*, *50*, 932–937.

Shang, C., & Barnabé, A. (2013). Structural study and phase transition investigation in a simple synthesis of porous architected-ZnO nanopowder. *Materials Characterization*, *86*, 206–211.

Sharma, D., & Jha, R. (2017). Structural and optical properties of Co-doped ZnO nano-ampoules synthesized by co-precipitation method. *Materials Letters*, *190*, 9–12.

Shi, R., Yang, P., Dong, X., Jia, C., & Li, J. (2014). Hydrothermal growth of upright-standing ZnO sheet microcrystals. *Materials Science and Engineering: B*, *186*, 68–72.

Sobana, N., & Swaminathan, M. (2007). Combination effect of ZnO and activated carbon for solar assisted photocatalytic degradation of Direct Blue 53. *Solar Energy Materials and Solar Cells*, *91*(8), 727–734.

Subash, B., Krishnakumar, B., Pandiyan, V., Swaminathan, M., & Shanthi, M. (2012). An efficient nanostructured Ag_2S–ZnO for degradation of Acid Black 1 dye under day light illumination. *Separation and Purification Technology*, *96*, 204–213.

Suntako, R. (2015). Effect of synthesized ZnO nanograins using a precipitation method for the enhanced cushion rubber properties. *Materials Letters*, *158*, 399–402.

Suwanboon, S., Amornpitoksuk, P., & Sukolrat, A. (2011). Dependence of optical properties on doping metal, crystallite size and defect concentration of M-doped ZnO nanopowders (M=Al, Mg, Ti). *Ceramics International*, *37*(4), 1359–1365.

Thanh Hoai Ta, Q., Park, S., & Noh, J.-S. (2017). Ag nanowire/ZnO nanobush hybrid structures for improved photocatalytic activity. *Journal of Colloid and Interface Science*, *505*, 437–444.

Thaweesaeng, N., Supankit, S., Techidheera, W., & Pecharapa, W. (2013). Structure Properties of As-synthesized Cu-doped ZnO Nanopowder Synthesized by Co-precipitation Method. *Energy Procedia*, *34*, 682–688.

Tran Thi, V. H., & Lee, B.-K. (2017). Great improvement on tetracycline removal using ZnO rod-activated carbon fiber composite prepared with a facile microwave method. *Journal of Hazardous Materials*, *324*, 329–339.

Vaiano, V., Matarangolo, M., Murcia, J. J., Rojas, H., Navío, J. A., & Hidalgo, M. C. (2018). Enhanced photocatalytic removal of phenol from aqueous solutions using ZnO modified with Ag. *Applied Catalysis B: Environmental*, *225*, 197–206.

Vinayagam, M., Ramachandran, S., Ramya, V., & Sivasamy, A. (2018). Photocatalytic degradation of orange G dye using ZnO/biomass activated carbon nanocomposite. *Journal of Environmental Chemical Engineering*, *6*(3), 3726–3734.

Wang, H., Qiu, X., Liu, W., & Yang, D. (2017). Facile preparation of well-combined lignin-based carbon/ZnO hybrid composite with excellent photocatalytic activity. *Applied Surface Science*, *426*, 206–216.

Wang, H., Li, C., Zhao, H., & Liu, J. (2013). Preparation of nano-sized flower-like ZnO bunches by a direct precipitation method. *Advanced Powder Technology*, *24*(3), 599–604.

Wang, Y., Zhang, C., Bi, S., & Luo, G. (2010). Preparation of ZnO nanoparticles using the direct precipitation method in a membrane dispersion micro-structured reactor. *Powder Technology*, *202*(1), 130–136.

Zamiri, R., Singh, B. K., Dutta, D., Reblo, A., & Ferreira, J. M. F. (2014). Electrical properties of Ag-doped ZnO nano-plates synthesized via wet chemical precipitation method. *Ceramics International*, *40*(3), 4471–4477.

Zhai, H., Wang, L., Sun, D., Han, D., Qi, B., Li, X., … Yang, J. (2015). Direct sunlight responsive Ag–ZnO heterostructure photocatalyst: Enhanced degradation of rhodamine B. *Journal of Physics and Chemistry of Solids*, *78*, 35–40.

Zhang, X., Wang, Y., Hou, F., Li, H., Yang, Y., Zhang, X., … Wang, Y. (2017). Effects of Ag loading on structural and photocatalytic properties of flower-like ZnO microspheres. *Applied Surface Science*, *391*, 476–483.

Zhao, X., Su, S., Wu, G., Li, C., Qin, Z., Lou, X., & Zhou, J. (2017). Facile synthesis of the flower-like ternary heterostructure of Ag/ZnO encapsulating carbon spheres with enhanced photocatalytic performance. *Applied Surface Science*, *406*, 254–264.

Zhong, J. bo, Xu, B., Feng, F. M., He, X. yang, Li, J. zhang, & Hu, W. (2011). Fabrication and photocatalytic activity of ZnO prepared by different precipitants using paralled flaw precipitation method. *Materials Letters*, *65*(12), 1995–1997.

VITAE

Neme Miss Khanitta Intarasuwan

Student ID 5710230028

Education Attainment

Degree	Name of Institution	Year of Graduation
M. Sc. (Chemistry)	Prince of Songkla University	2013
B. Sc. (Chemistry)	Prince of Songkla University	2009

Scholarship Awards during Enrolment

1. PSU Ph.D. Scholarship
2. Graduate School, Prince of Songkla University

List of Publication

1. Intarasuwan, K., Amornpitoksuk, P., Suwanboon, S., & Graidist, P. (2017). Photocatalytic dye degradation by ZnO nanoparticles prepared from $X_2C_2O_4$ (X=H, Na and NH_4) and the cytotoxicity of the treated dye solutions. *Separation and Purification Technology*, *177*, 304–312.

2. Intarasuwan, K., Amornpitoksuk, P., Suwanboon, S., Graidist, P., Maungchanburi, S., & Randorn, C. (2018). Effect of Ag loading on activated carbon doped ZnO for bisphenol A degradation under visible light. *Advanced Powder Technology*, *29*(11), 2608–2615.

Title: Photocatalytic dye degradation by ZnO nanoparticles prepared from X2C2O4 (X=H, Na and NH4) and the cytotoxicity of the treated dye solutions

Author: Khanitta Intarasuwan,Pongsaton Amornpitoksuk,Sumetha Suwanboon,Potchanapond Graidist

Publication: Separation and Purification Technology

Publisher: Elsevier

Date: 28 April 2017

Please note that, as the author of this Elsevier article, you retain the right to include it in a thesis or dissertation, provided it is not published commercially. Permission is not required, but please ensure that you reference the journal as the original source. For more information on this and on your other retained rights, please visit: https://www.elsevier.com/about/our-business/policies/copyright#Author-rights

Title: Effect of Ag loading on activated carbon doped ZnO for bisphenol A degradation under visible light

Author: Khanitta Intarasuwan,Pongsaton Amornpitoksuk,Sumetha Suwanboon,Potchanapond Graidist,Saowanee Maungchanburi,Chamnan Randorn

Publication: Advanced Powder Technology

Publisher: Elsevier

Date: November 2018

Please note that, as the author of this Elsevier article, you retain the right to include it in a thesis or dissertation, provided it is not published commercially. Permission is not required, but please ensure that you reference the journal as the original source. For more information on this and on your other retained rights, please visit: https://www.elsevier.com/about/our-business/policies/copyright#Author-rights